

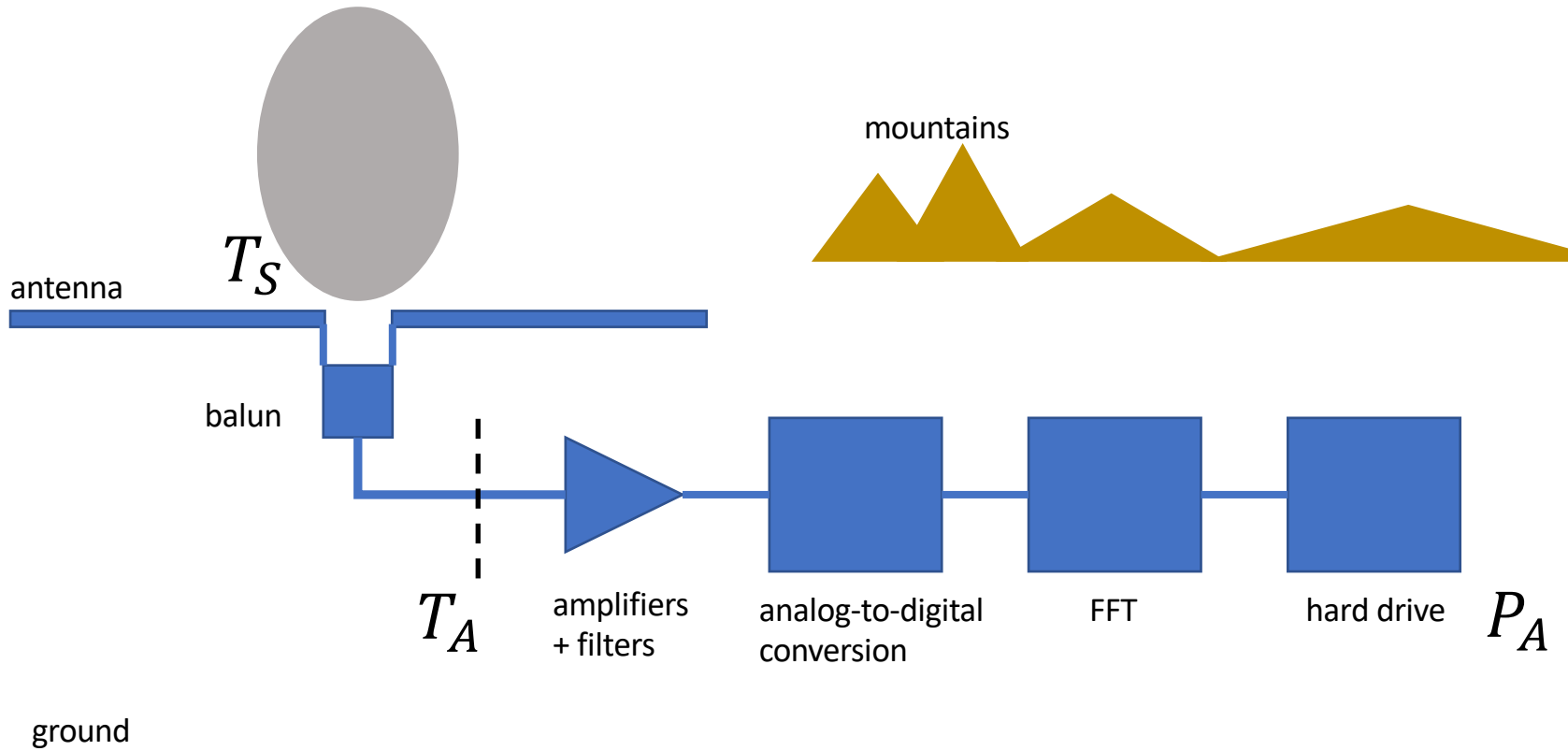
Status of 21-cm Global Signal

Raul Monsalve



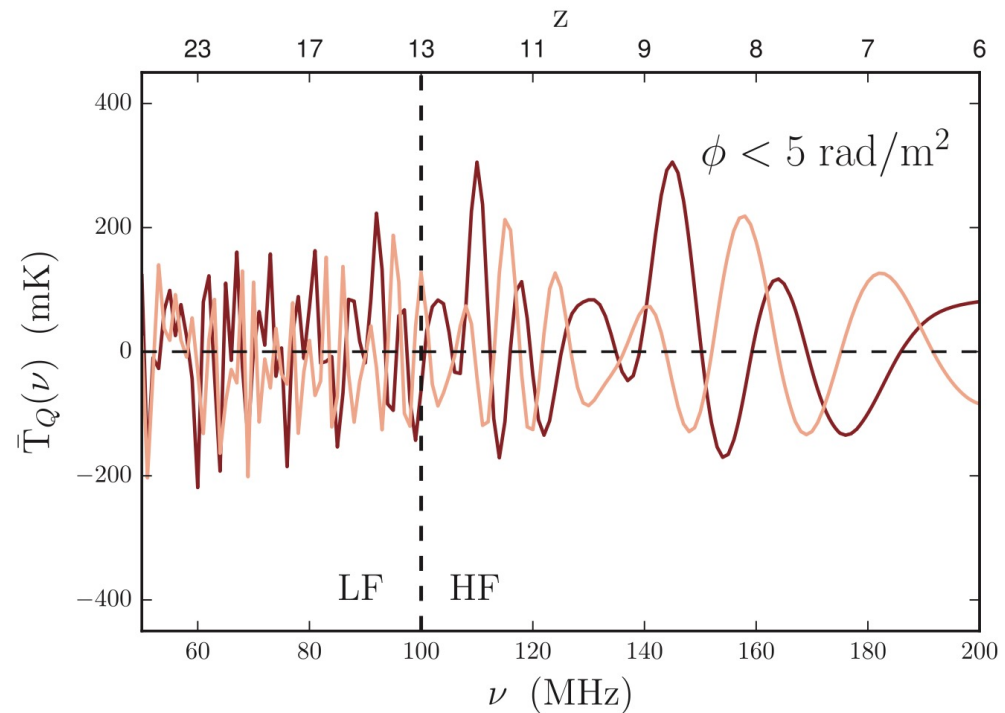
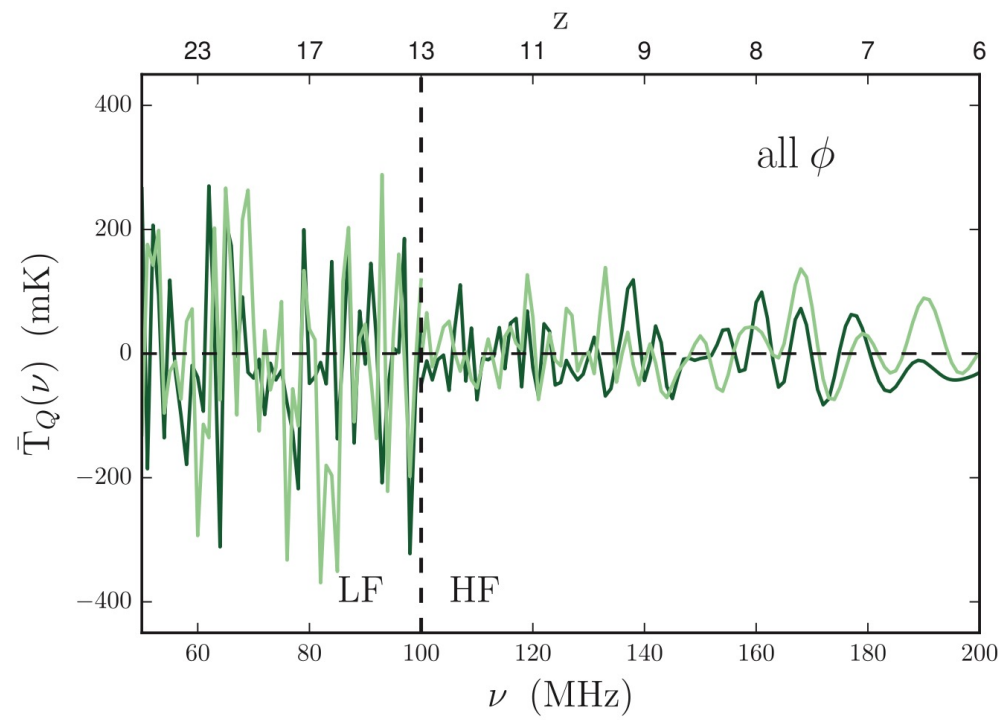
Redshifted 21-cm signal

- Unpolarized diffuse foreground
- Polarized diffuse foreground
- Ionospheric attenuation, emission, and refraction
- Tropospheric refraction



Polarized Foregrounds

Spinelli, Bernardi, Santos (2019)



Next:

Instrumental Stuff

Receiver Calibration

$$T_A(\nu) = \frac{P_A(\nu)}{g_R(\nu)} - T_R(\nu)$$

- Receiver gain and temperature
- Typically obtained from lab and field measurements of calibration standards
- Impedance mismatch between antenna and receiver input

(for single-polarization antenna)

$$T_S(\nu) = \frac{\int_0^{2\pi} \int_0^{\pi/2} T_{sky}(\theta, \phi, \nu) D(\theta, \phi, \nu) \sin \theta d\theta d\phi}{\int_0^{2\pi} \int_0^{\pi/2} D(\theta, \phi, \nu) \sin \theta d\theta d\phi}$$

Beam Chromaticity Correction

$$C(\nu, t) = \left(\frac{\int_0^{2\pi} \int_0^{\pi/2} T_{GSM}(\theta, \phi, \nu, t) D_c(\theta, \phi, \nu) \sin \theta d\theta d\phi}{\int_0^{2\pi} \int_0^{\pi/2} D_c(\theta, \phi, \nu) \sin \theta d\theta} \right) \times \left(\frac{\int_0^{2\pi} \int_0^{\pi/2} T_{GSM}(\theta, \phi, \nu, t) D_c(\theta, \phi, \nu_r) \sin \theta d\theta d\phi}{\int_0^{2\pi} \int_0^{\pi/2} D_c(\theta, \phi, \nu_r) \sin \theta d\theta} \right)^{-1}$$

Measurement Efficiency (1- Losses)

$$T_A(\nu) = \eta(\nu)T_S(\nu) + [1 - \eta(\nu)] T_{phys}$$

$$T_S = \frac{T_A - [1 - \eta_{rad}\eta_{beam}\eta_{balun}] T_{phys}}{\eta_{rad}\eta_{beam}\eta_{balun}}$$

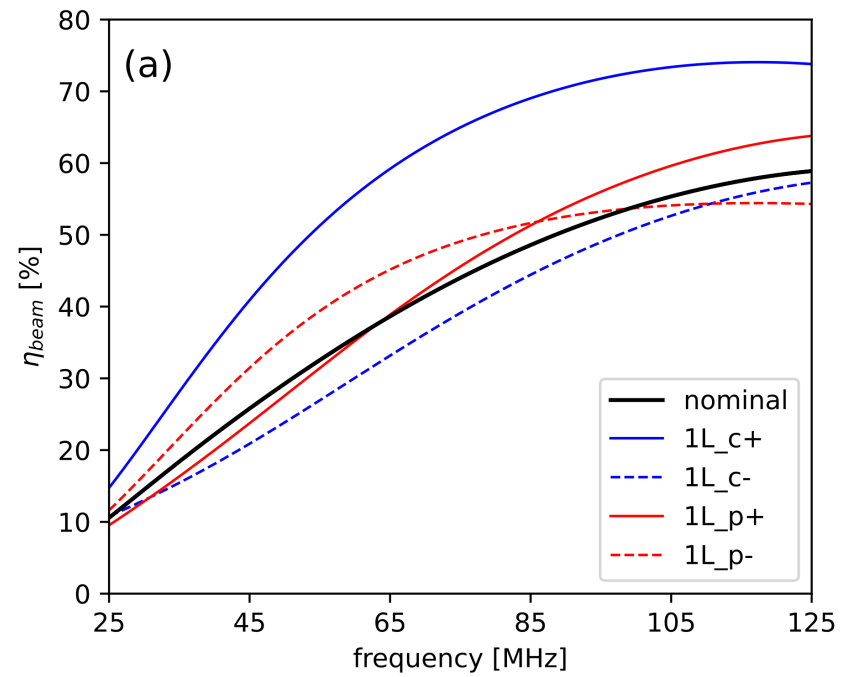
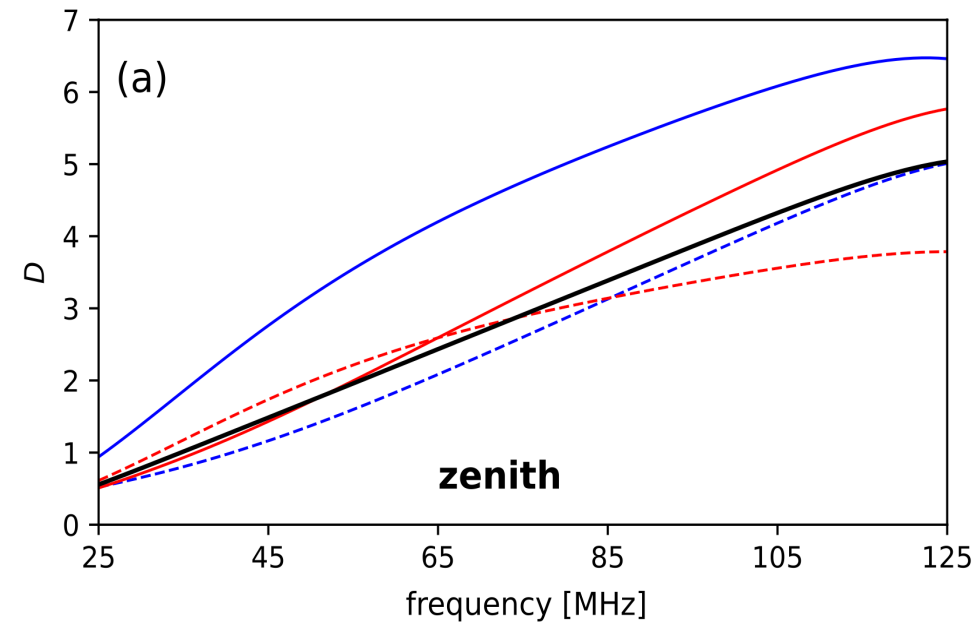
Radiation Efficiency

$$G(\theta, \phi, \nu) = \eta_{rad}(\nu)D(\theta, \phi, \nu)$$

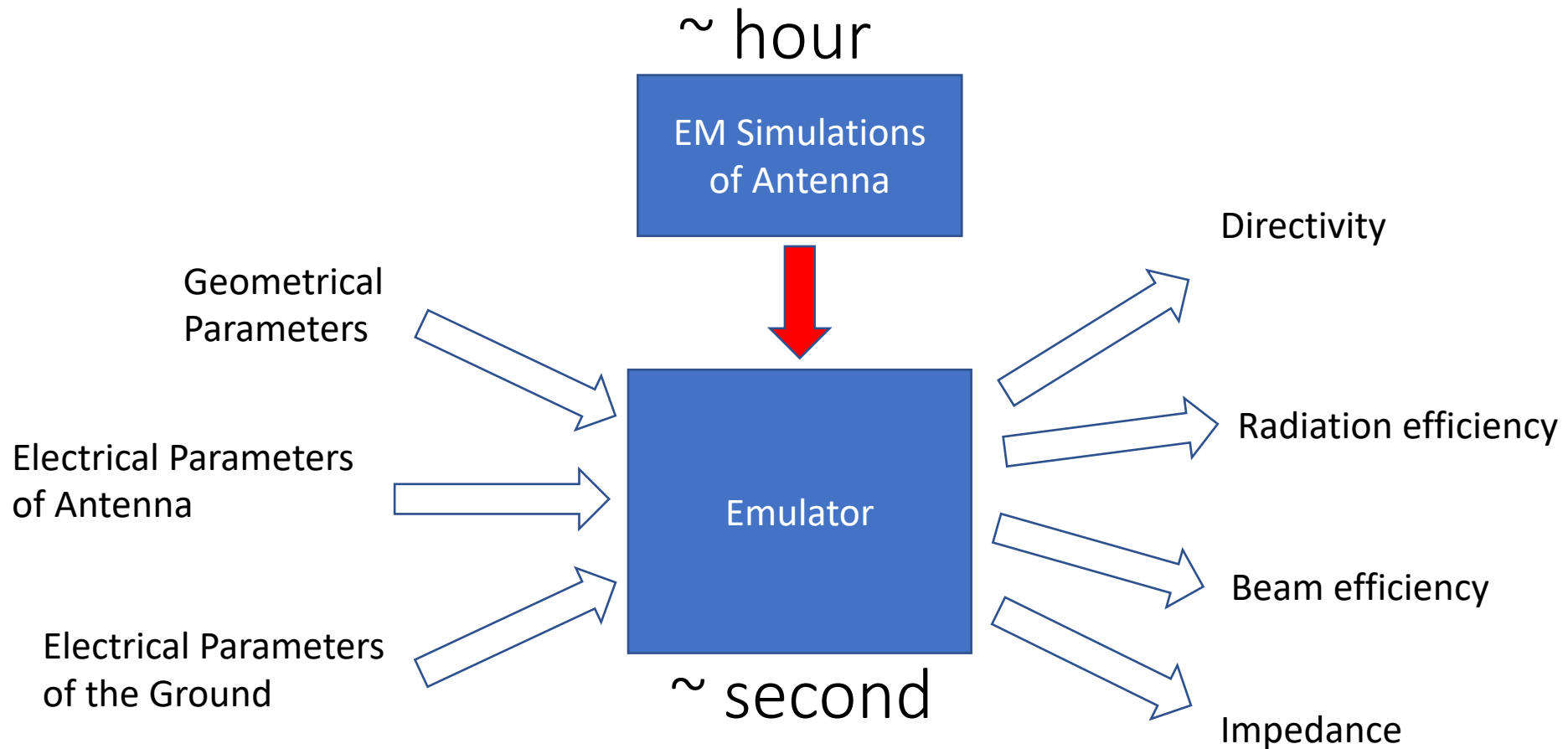
Beam Efficiency

$$\eta_{beam}(\nu) = \frac{1}{4\pi} \int_0^{2\pi} \int_0^{\pi/2} D(\theta, \phi, \nu) \sin \theta d\theta d\phi$$

Sensitivity of the Ground



Urgently Needed: Accurate Emulator of Antenna Performance



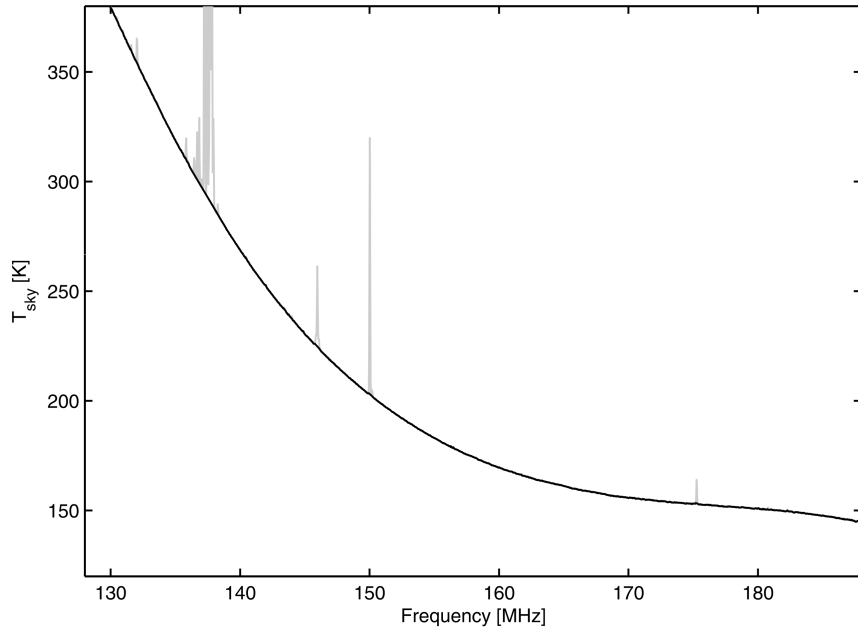
Next:

Data Calibrated Differently

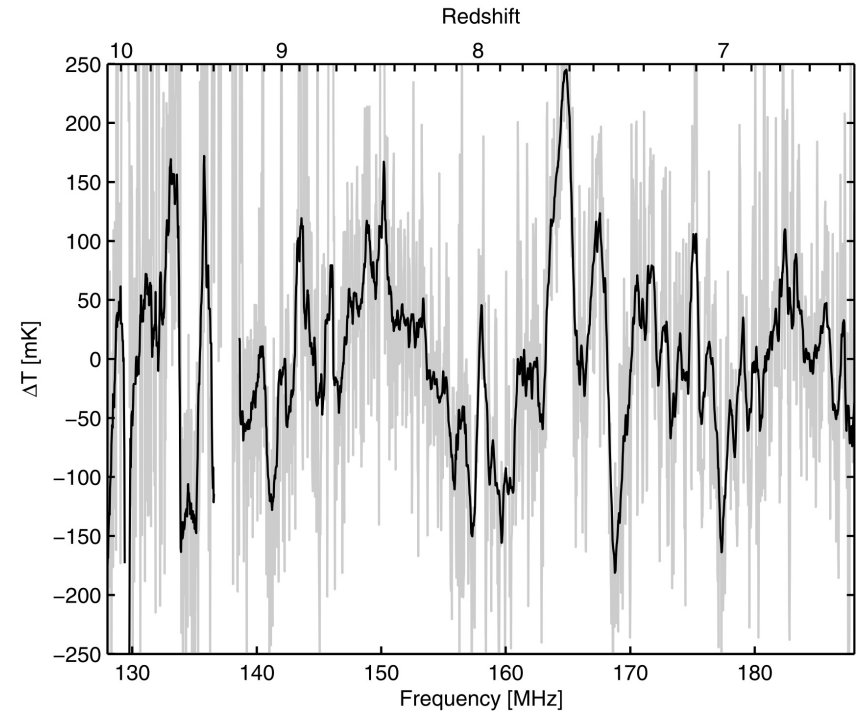
Models Constraints Differently

Results Reported Differently

Bowman, Rogers, Hewitt (2008) - EDGES



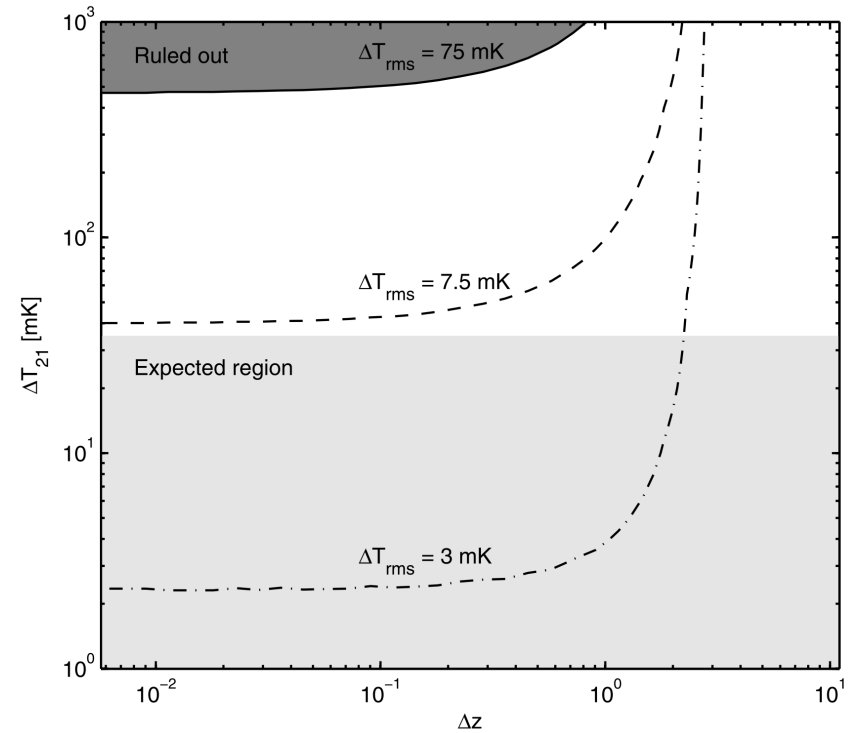
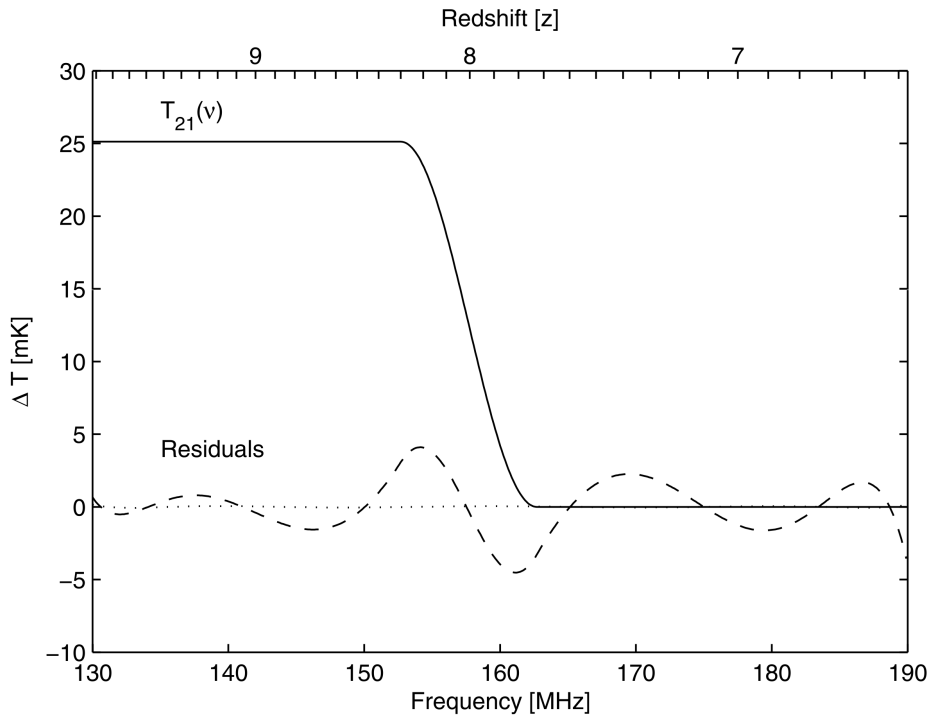
- ~4 hours of observations
- 3-position switching
- 130 – 190 MHz



- 8-term polynomial
- 75 mK residuals (after smoothing)

Bowman, Rogers, Hewitt (2008) - EDGES

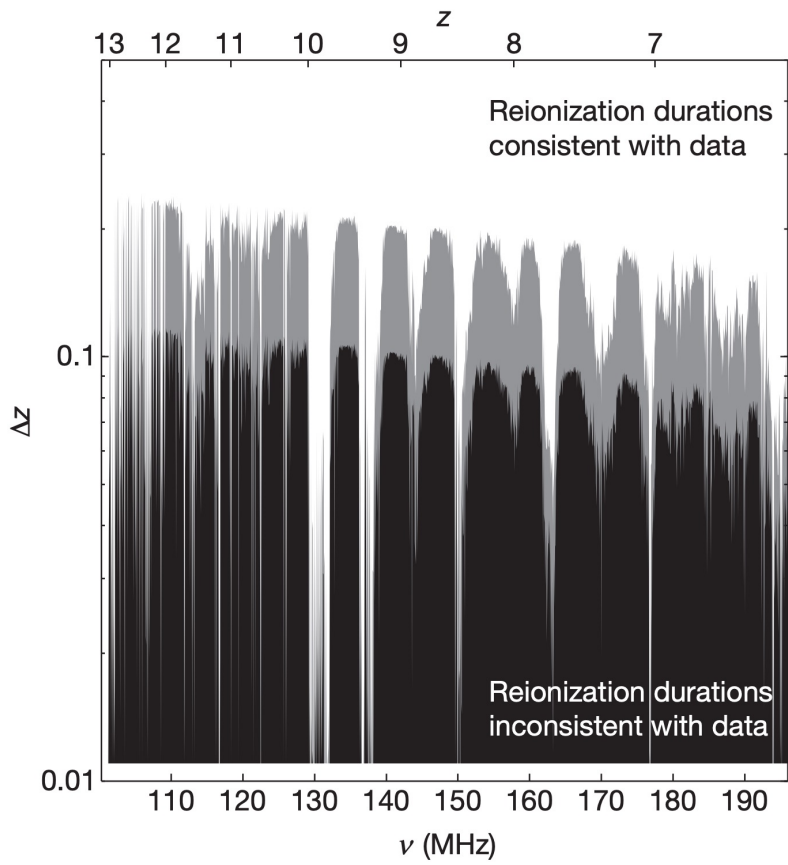
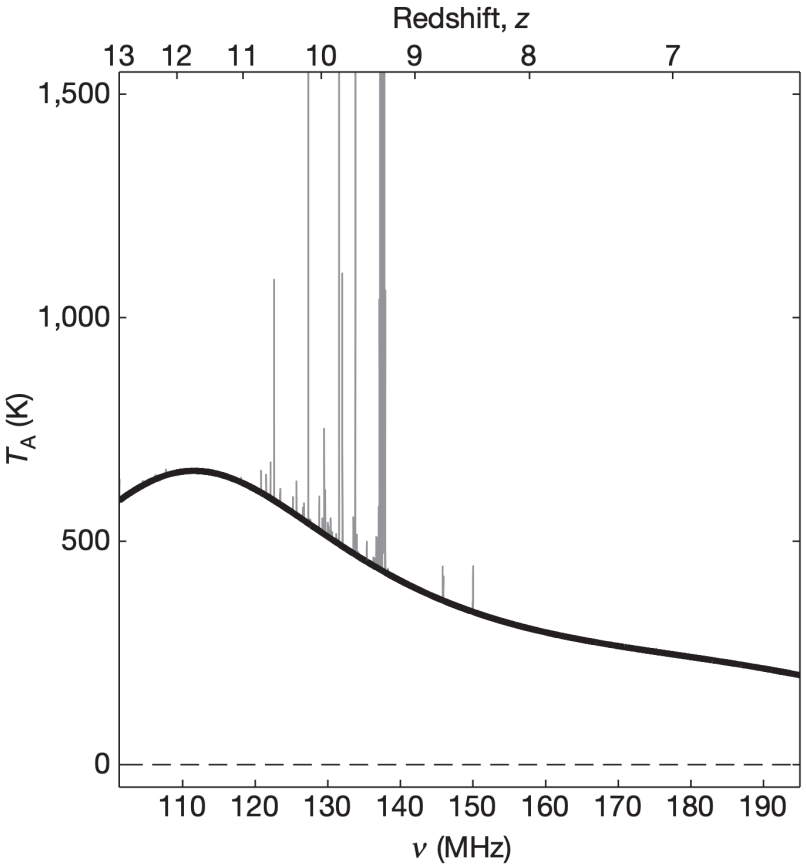
$$T_{21}(z) = \Delta T_{21} \frac{1}{2} \left\{ 1 + \cos \left[\frac{\pi(z_r - z - \Delta z/2)}{\Delta z} \right] \right\}$$



- Analytical EoR model centered at $z=8$
- Amplitude and duration varied

Bowman and Rogers (2010) -EDGES

$$\delta \bar{T}_{21}(z) \approx 27 \left(\frac{1+z}{10} \right)^{1/2} \bar{x}_{HI}(z) \text{ mK} \quad \tilde{x}_{HI}(z) = \frac{1}{2} \left[\tanh \left(\frac{z-z_r}{\Delta z} \right) + 1 \right]$$



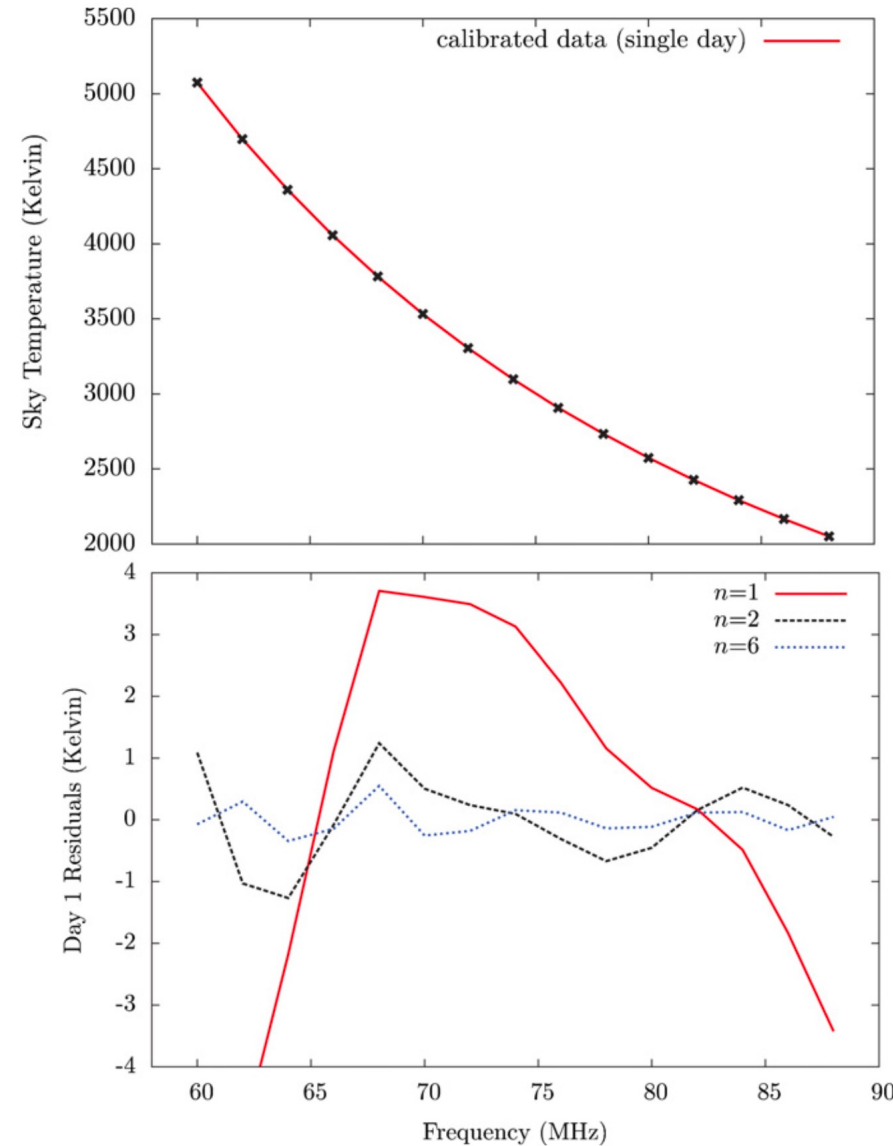
- 3 months of observations
- Noise 6 mK at 150 MHz and 1 MHz

- Sweeping 20 MHz windows
- Fitting 5 or 6 term polynomials + 21 cm signal
- 21-cm transition centered at νr
- Amplitude fixed, free parameter only duration

Voytek et al. (2014) -SCI-HI

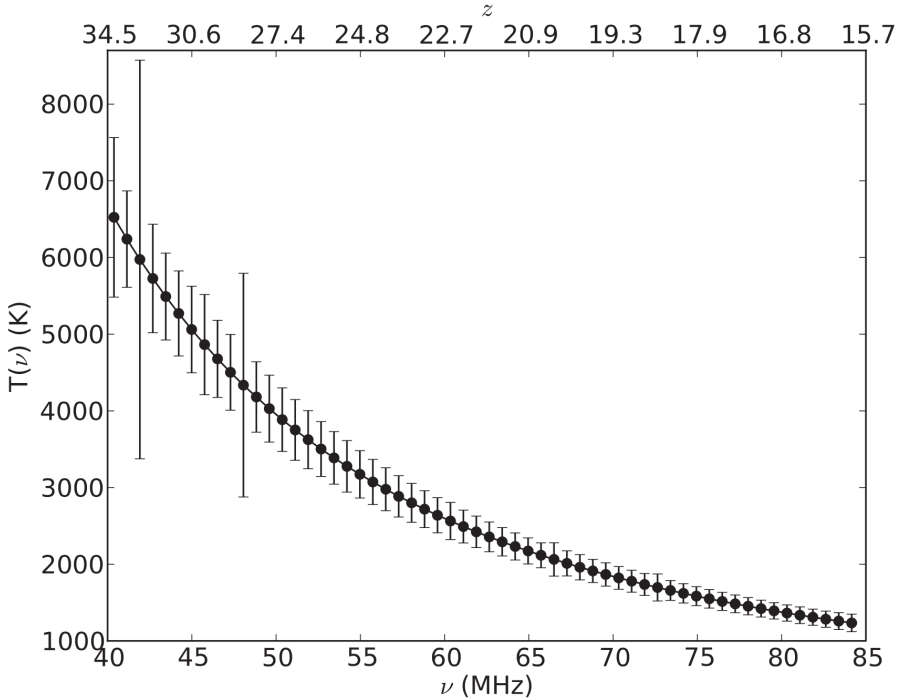
- 60-87 MHz (Lowest frequencies to date)
- 50-minute integration per day
- 9 days of data
- 2-MHz resolution
- 3 calibration approaches (2 approaches using Global Sky Model)
- 3-term Log-Log foreground model

$$\log_{10} T_{\text{GM}}(\nu) = \sum_{k=0}^n a_k \left[\log_{10} \left(\frac{\nu}{70 \text{ MHz}} \right) \right]^k$$

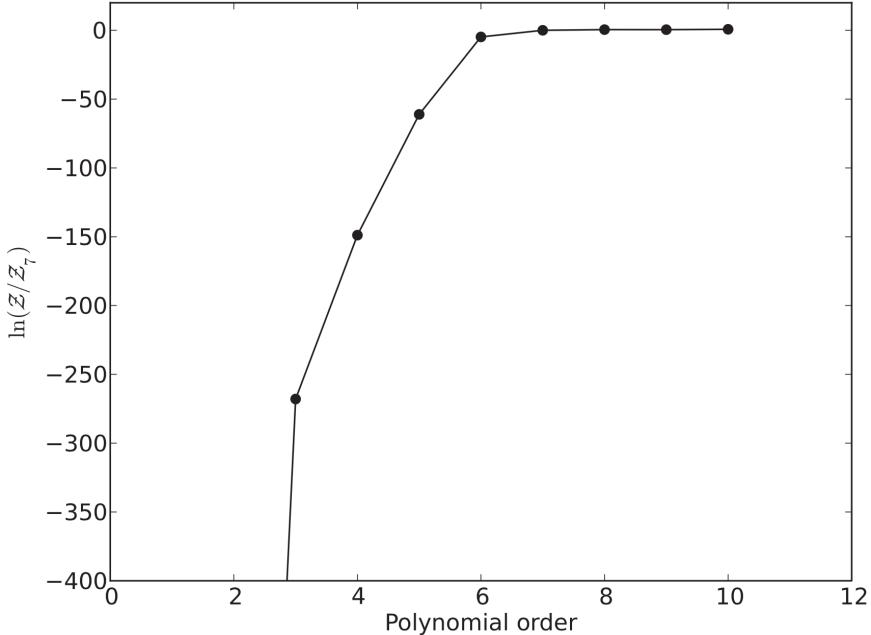


Bernardi et al. (2016)

-LEDA

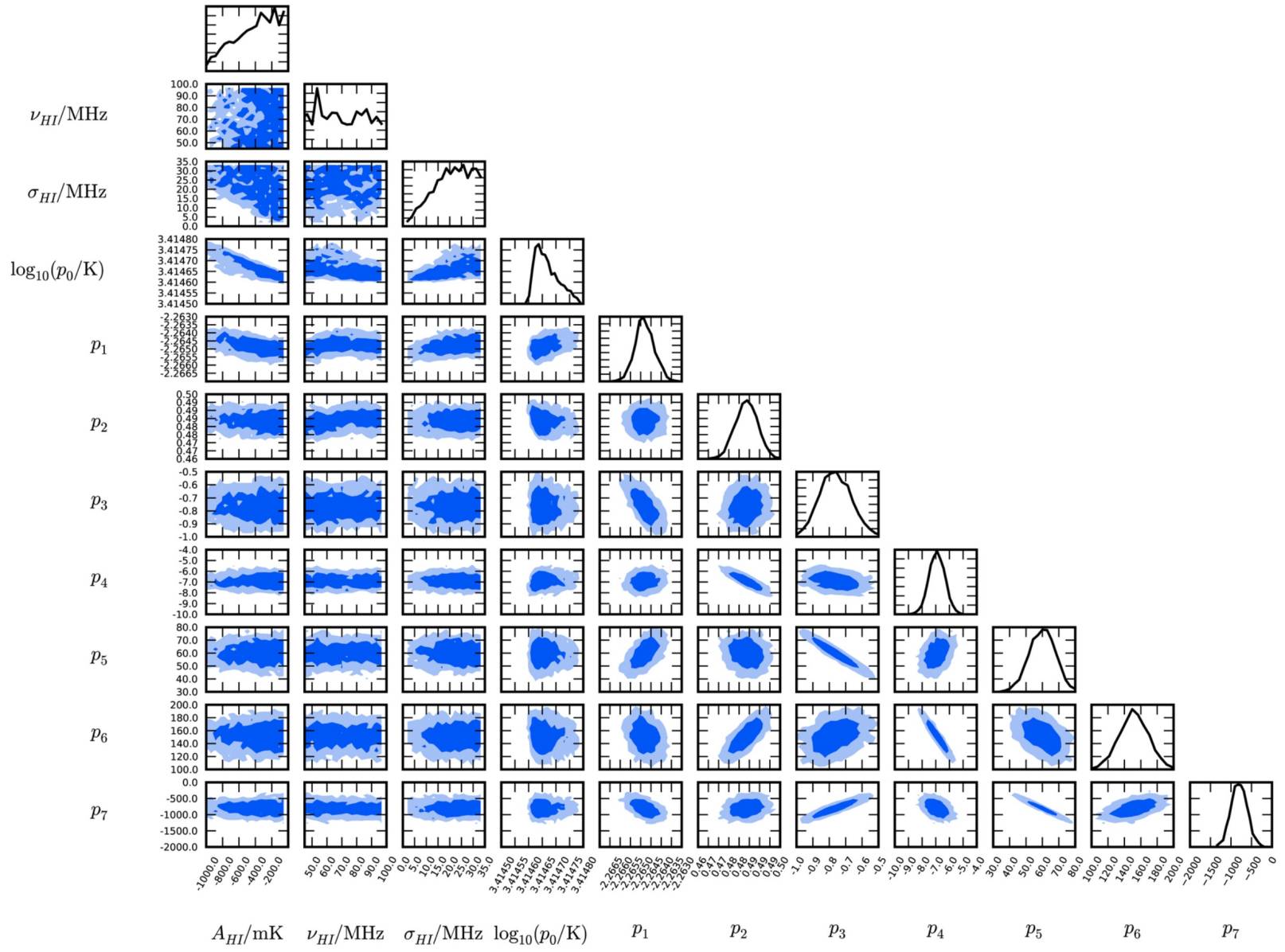


2-h of data (19-minute effective integration time)

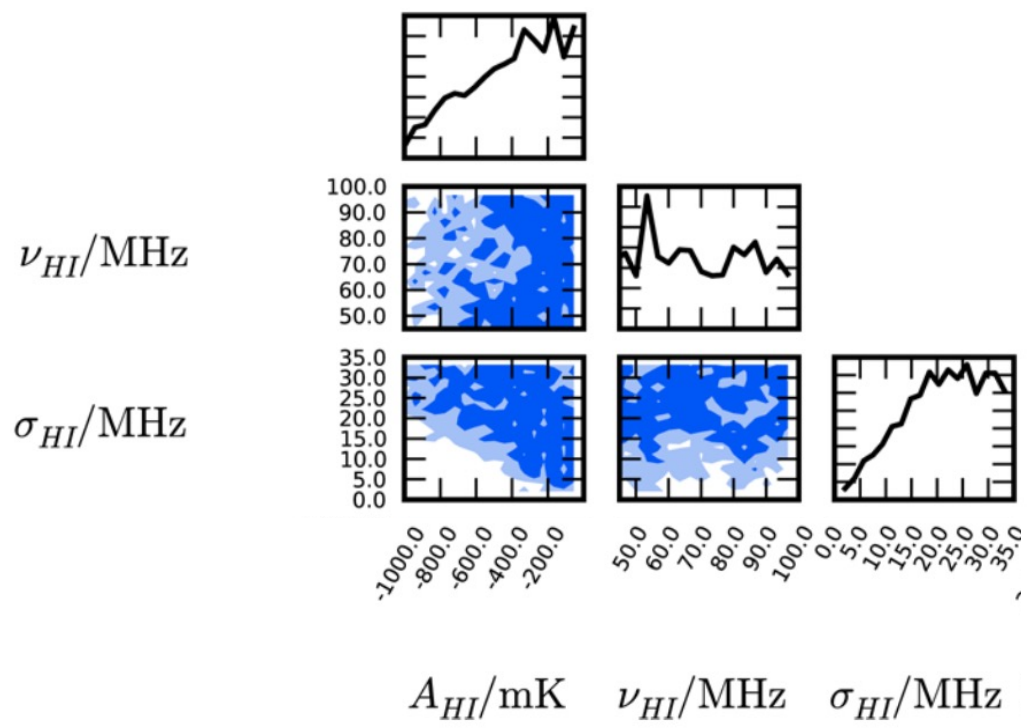


- 50-85 MHz
- Gaussian model for cosmic dawn feature
- 8-term log-log polynomial
- Bayesian analysis

Bernardi et al. (2016) -LEDA



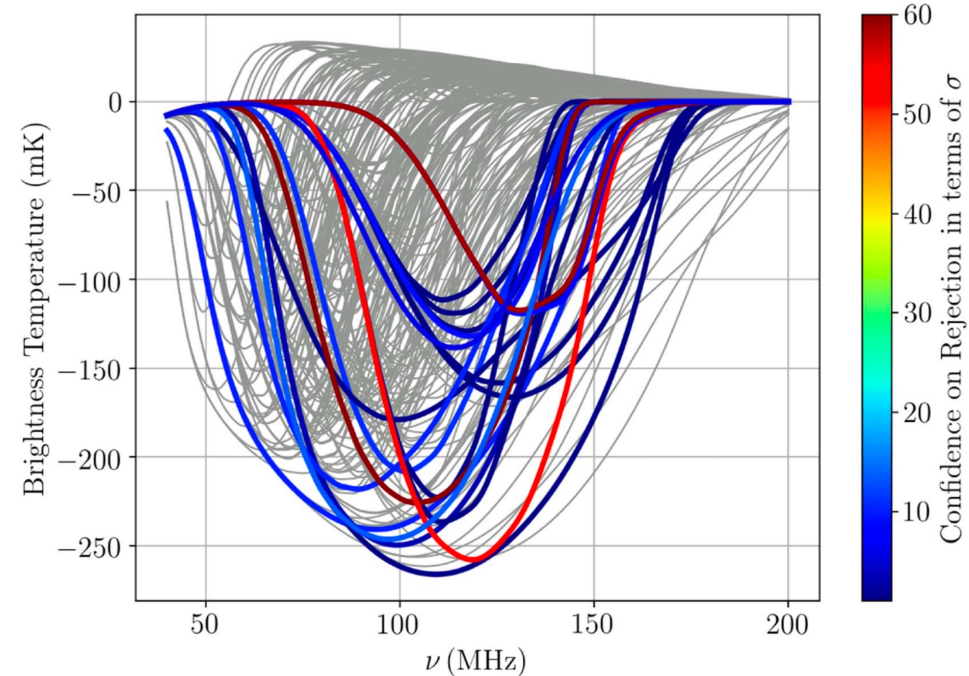
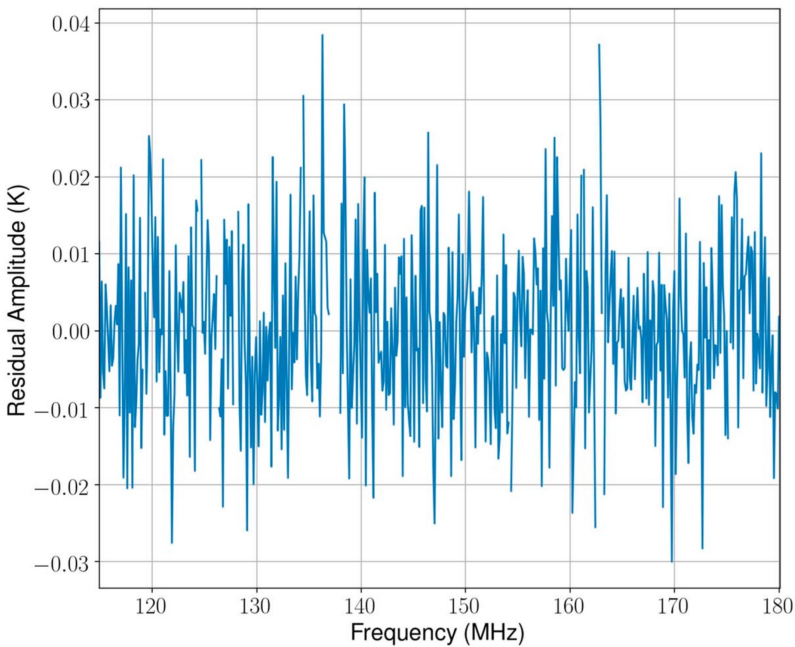
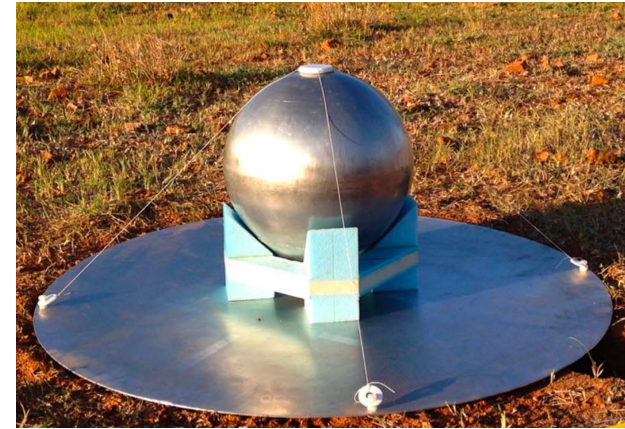
Bernardi et al. (2016) -LEDA



$-890 < A_{HI} < 0 \text{ mK}$ and $\sigma_{HI} > 6.5 \text{ MHz}$ at 95% confidence

Singh et al. (2017,2018) -SARAS 2

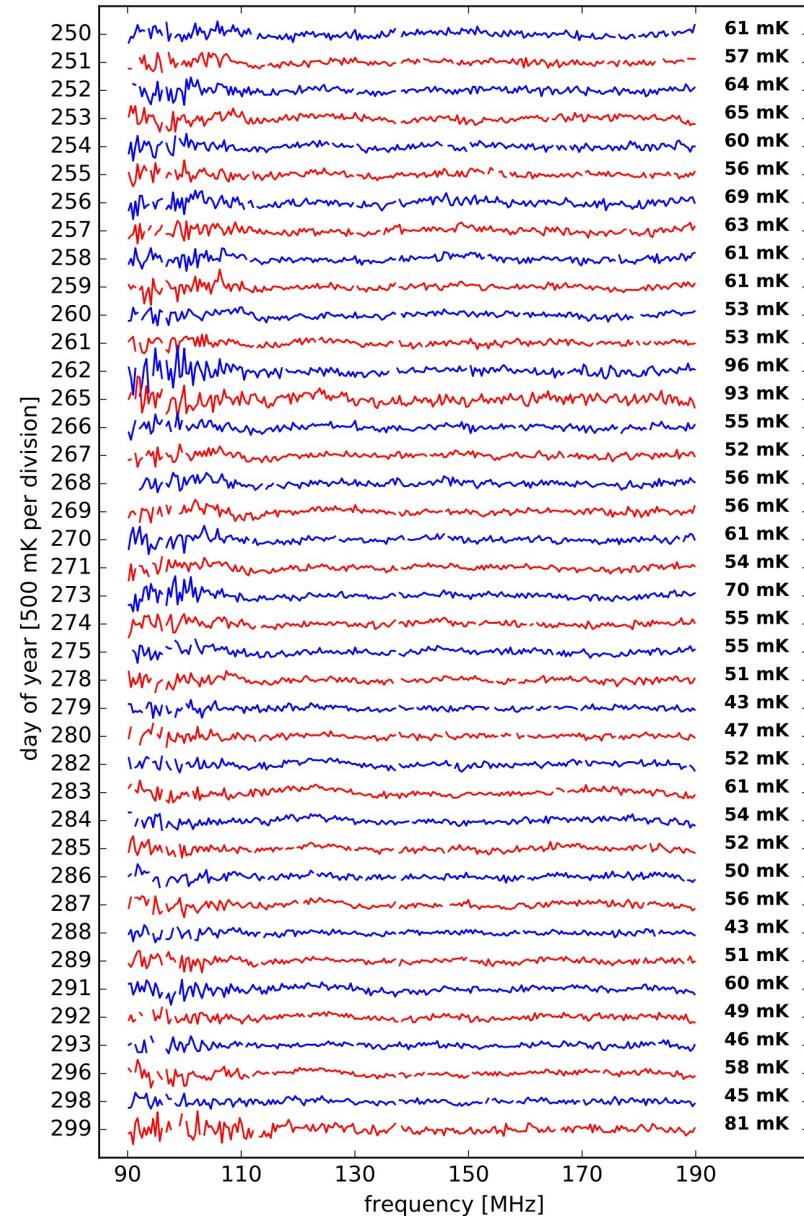
- Spherical monopole antenna
- Correlation spectrometer
- Estimating the total efficiency using GMOSS foreground model
- 63 h of data
- Removing polynomial within range 110-200 MHz
- Probing semi-numerical models from Cohen et al (2017)
- 2 methods: Likelihood ratio and fitting a scale



Monsalve et al. (2017,2018,2019)

EDGES High-Band

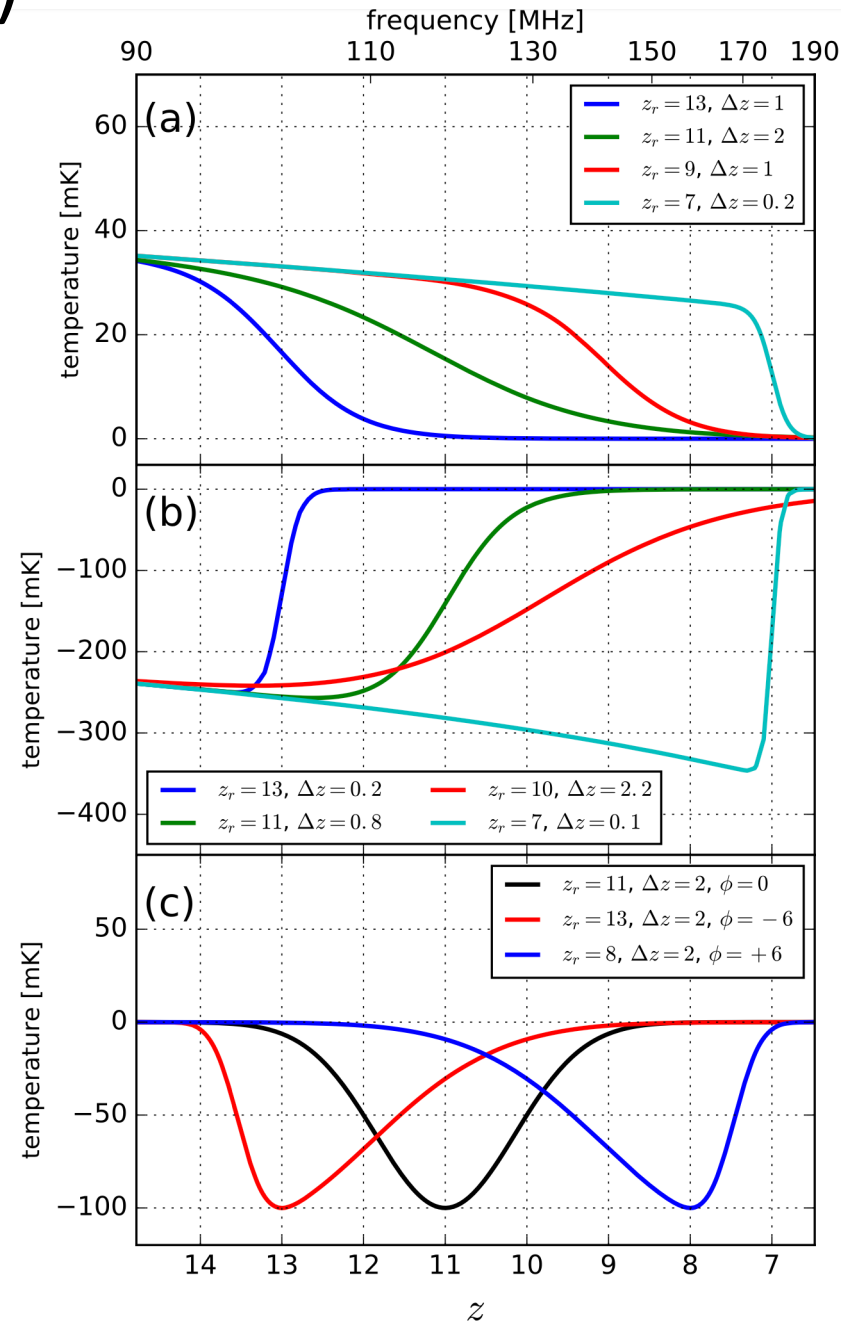
$$\hat{T}_{\text{fg}}(\nu) = \sum_{i=0}^4 a_i \nu^{-2.5+i}$$



Monsalve et al. (2017)

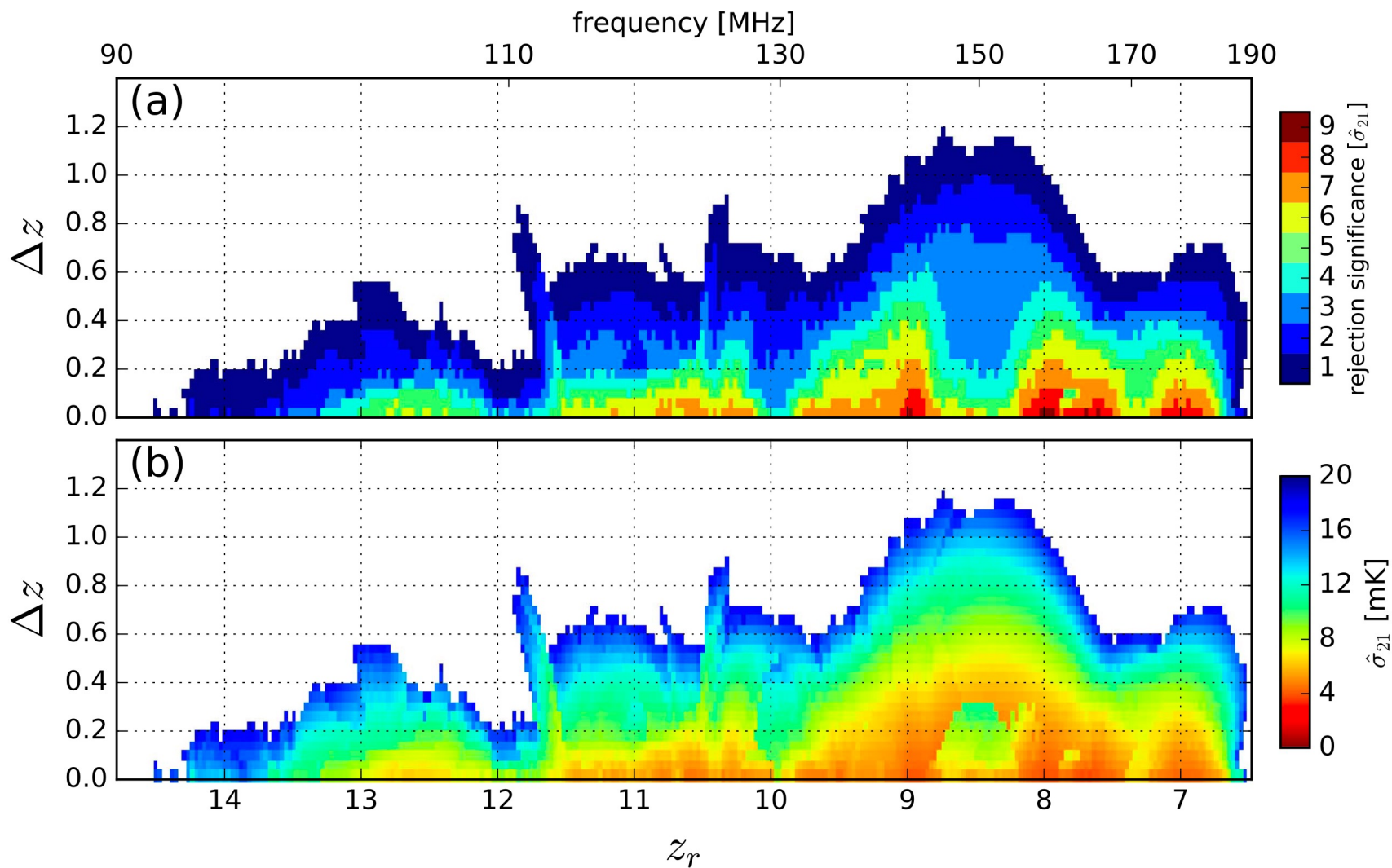
EDGES High-Band

- Phenomenological signals
- Hot EoR, Tanh evolution of neutral fraction
- Cold EoR, Tanh evolution, strong Ly-alpha, NO IGM heating, only EoR. Provided by Jordan Mirocha
- Gaussian absorption models, with and without asymmetry



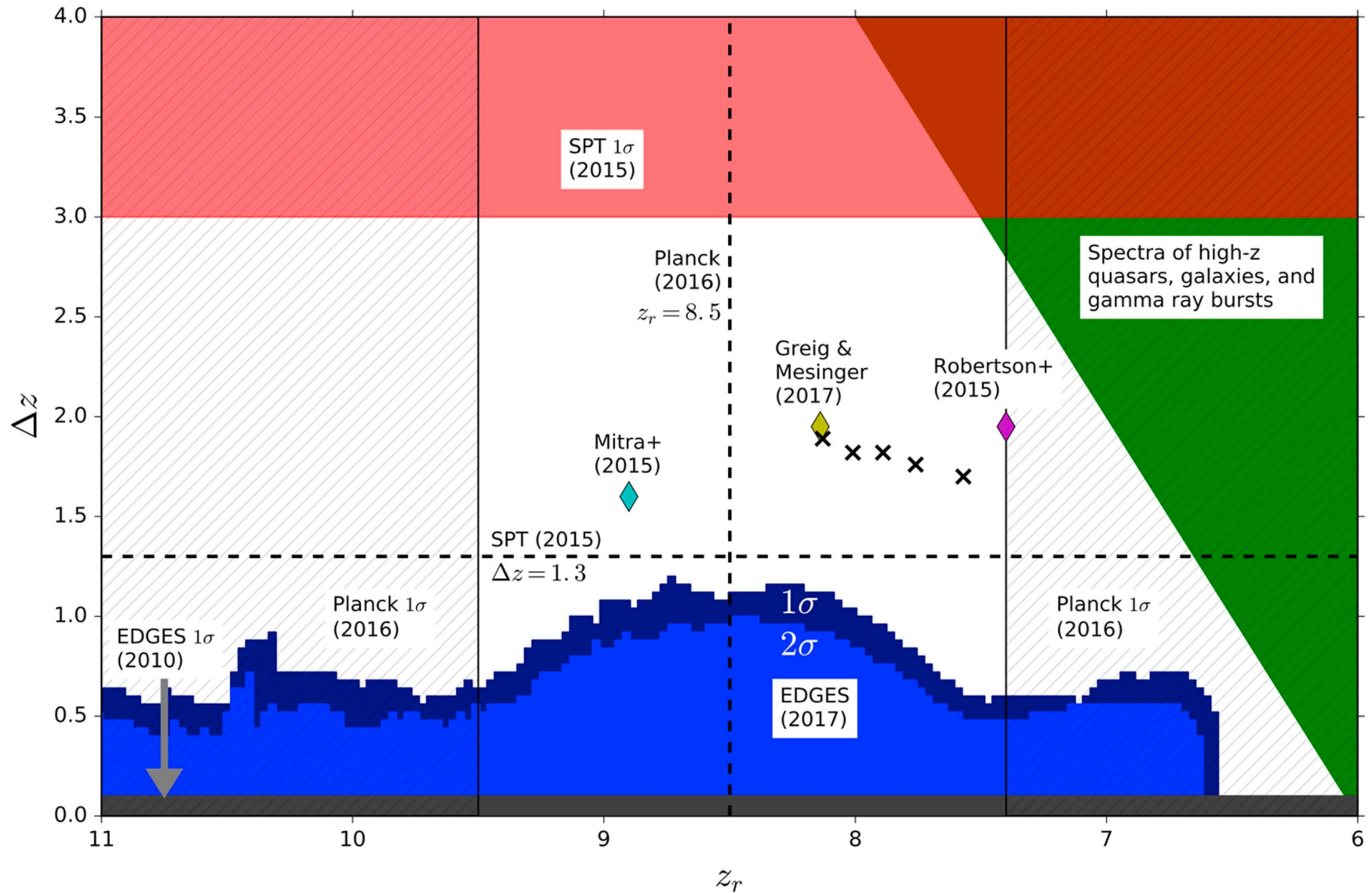
Monsalve et al. (2017)

EDGES High-Band



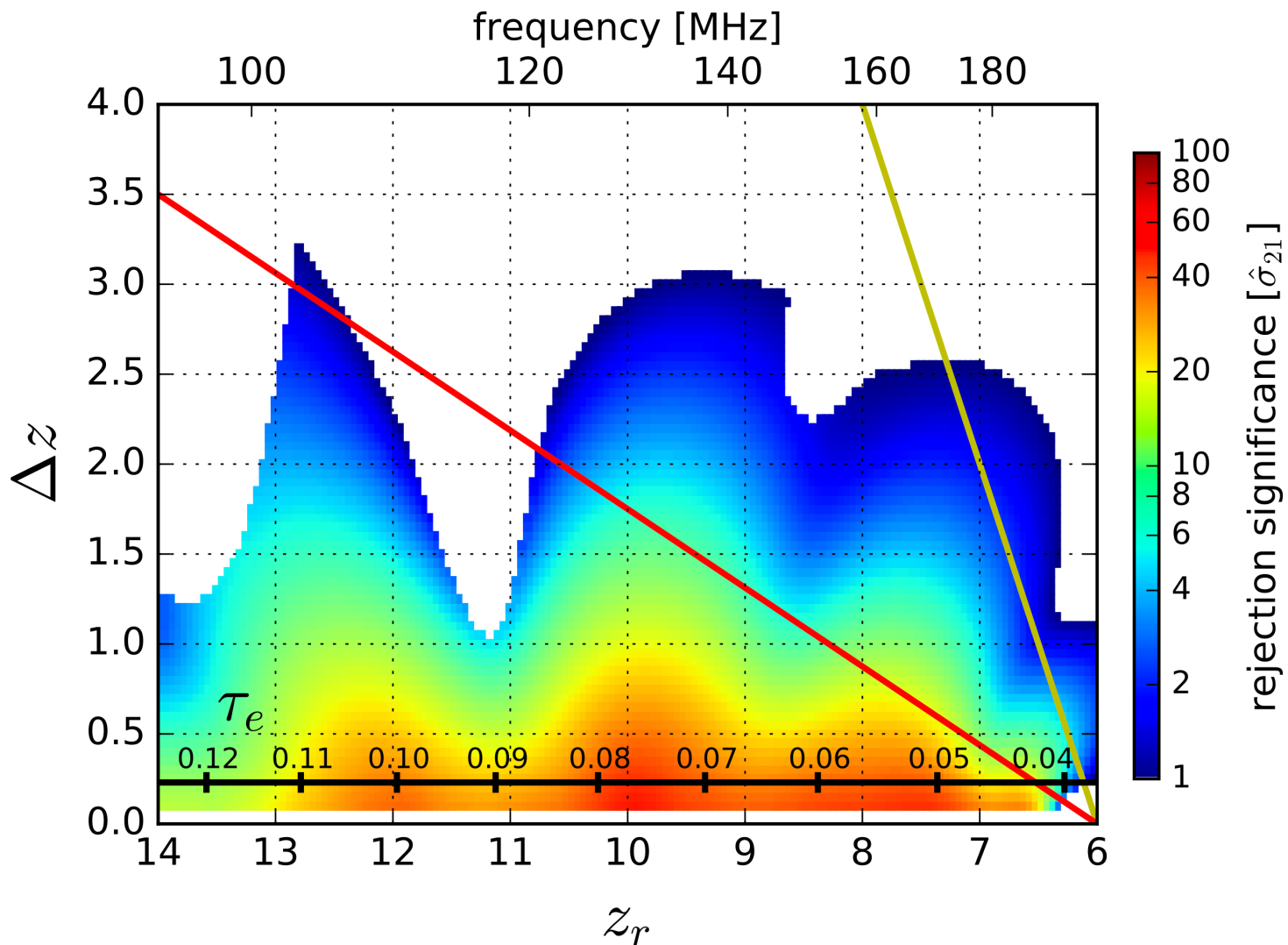
Monsalve et al. (2017)

EDGES High-Band



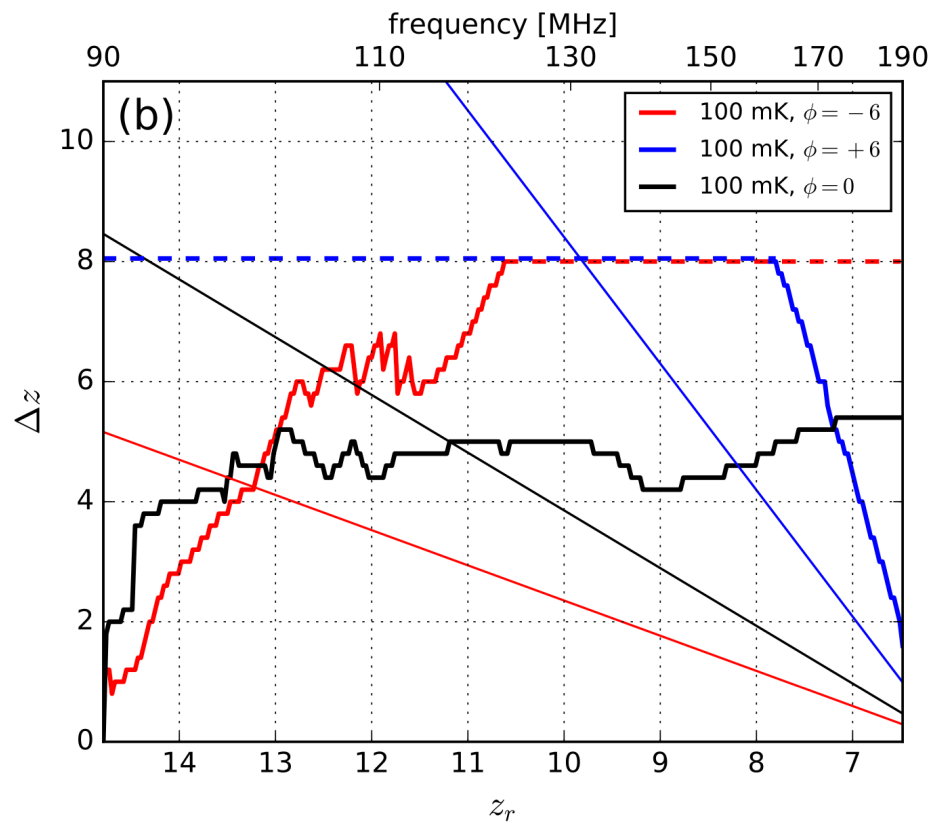
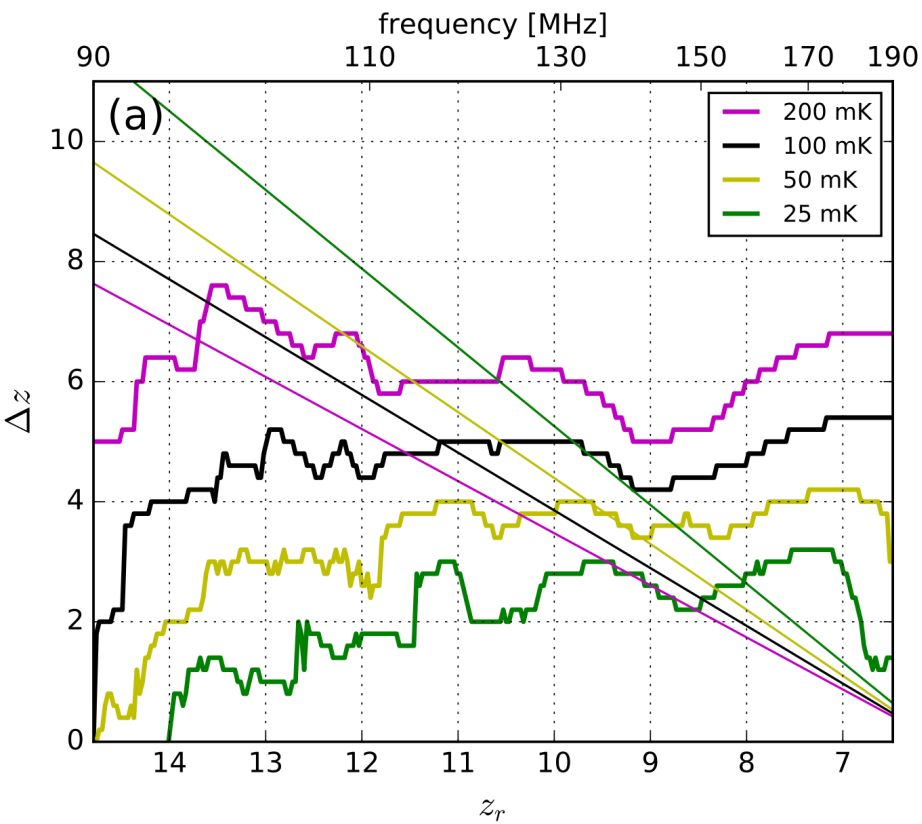
Monsalve et al. (2017)

EDGES High-Band



Monsalve et al. (2017)

EDGES High-Band

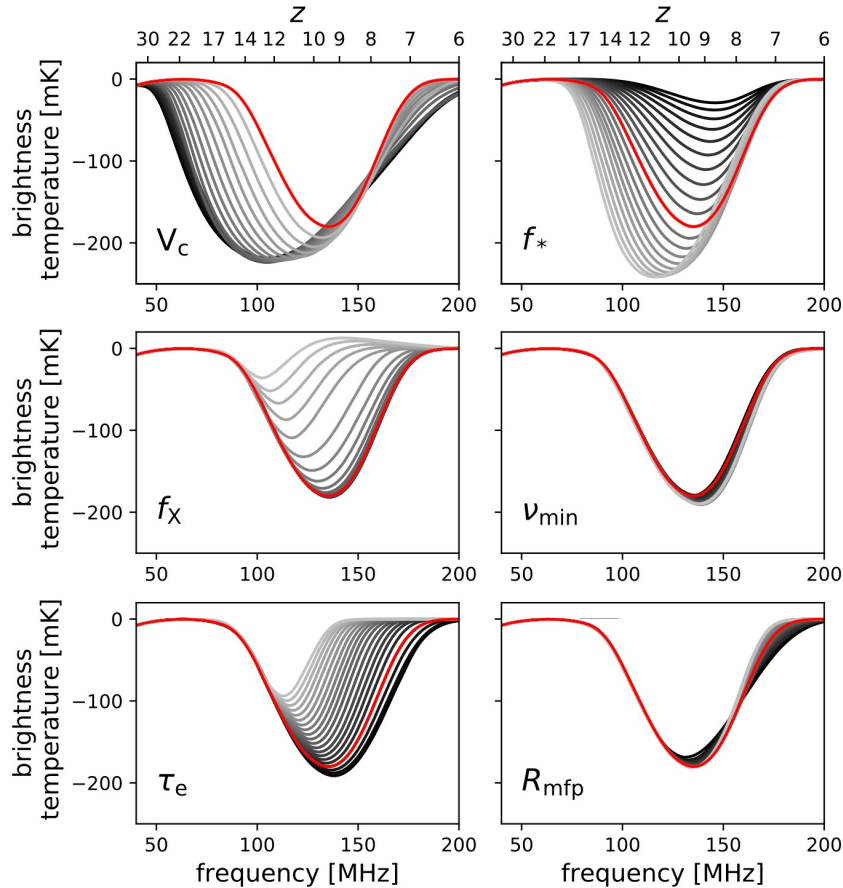


Monsalve, Fialkov, et al. (2019)

EDGES High-Band

21cmGEM

$$\hat{T}_{\text{fg}}(\nu) = \sum_{i=0}^4 a_i \nu^{-2.5+i}$$



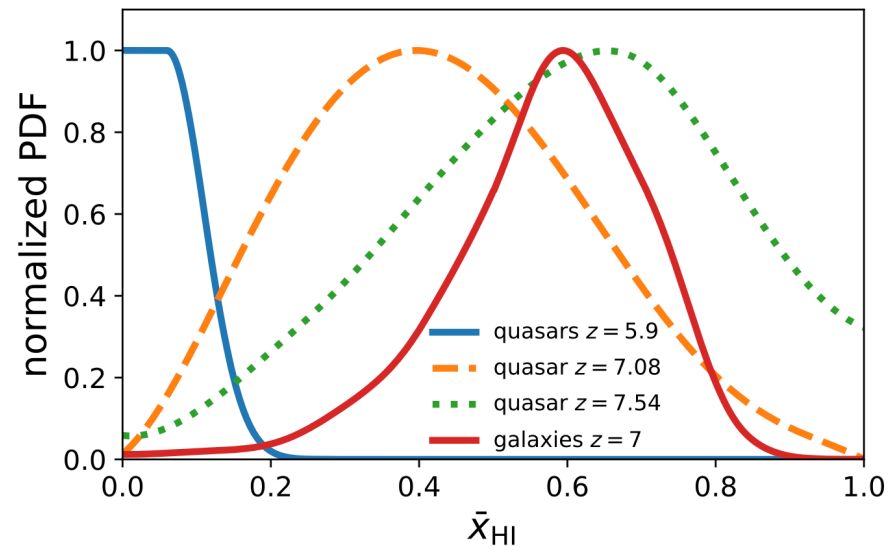
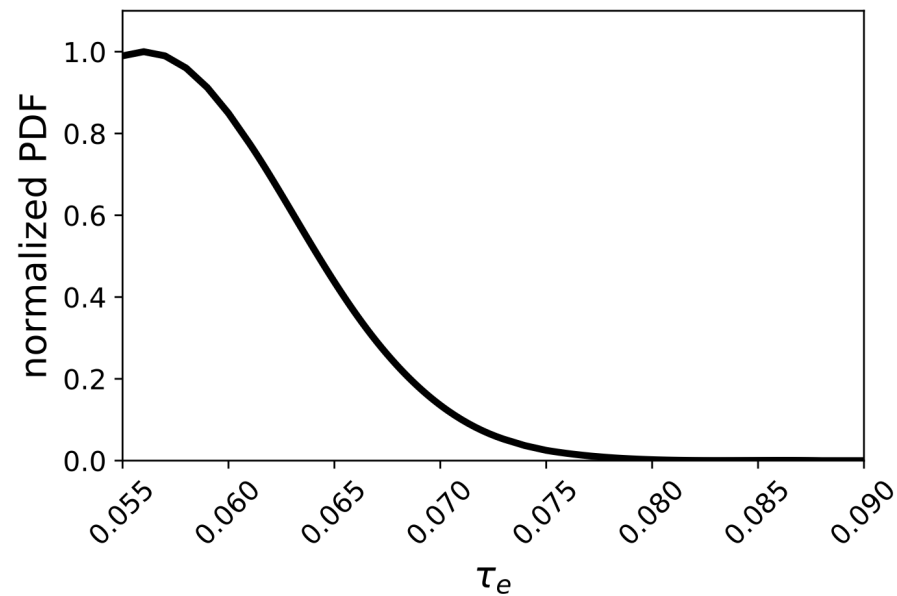
Parameter Ranges and Sampling Scale

Parameter	Min	Max	Unit	Scale
V_c	4.2	76.5	km s^{-1}	\log_{10}
f_*	10^{-3}	0.5	...	\log_{10}
f_X	10^{-5}	10	...	\log_{10}
ν_{\min}	0.1	3	keV	linear
τ_e	0.055	0.09	...	linear
R_{mfp}	10	50	Mpc	linear

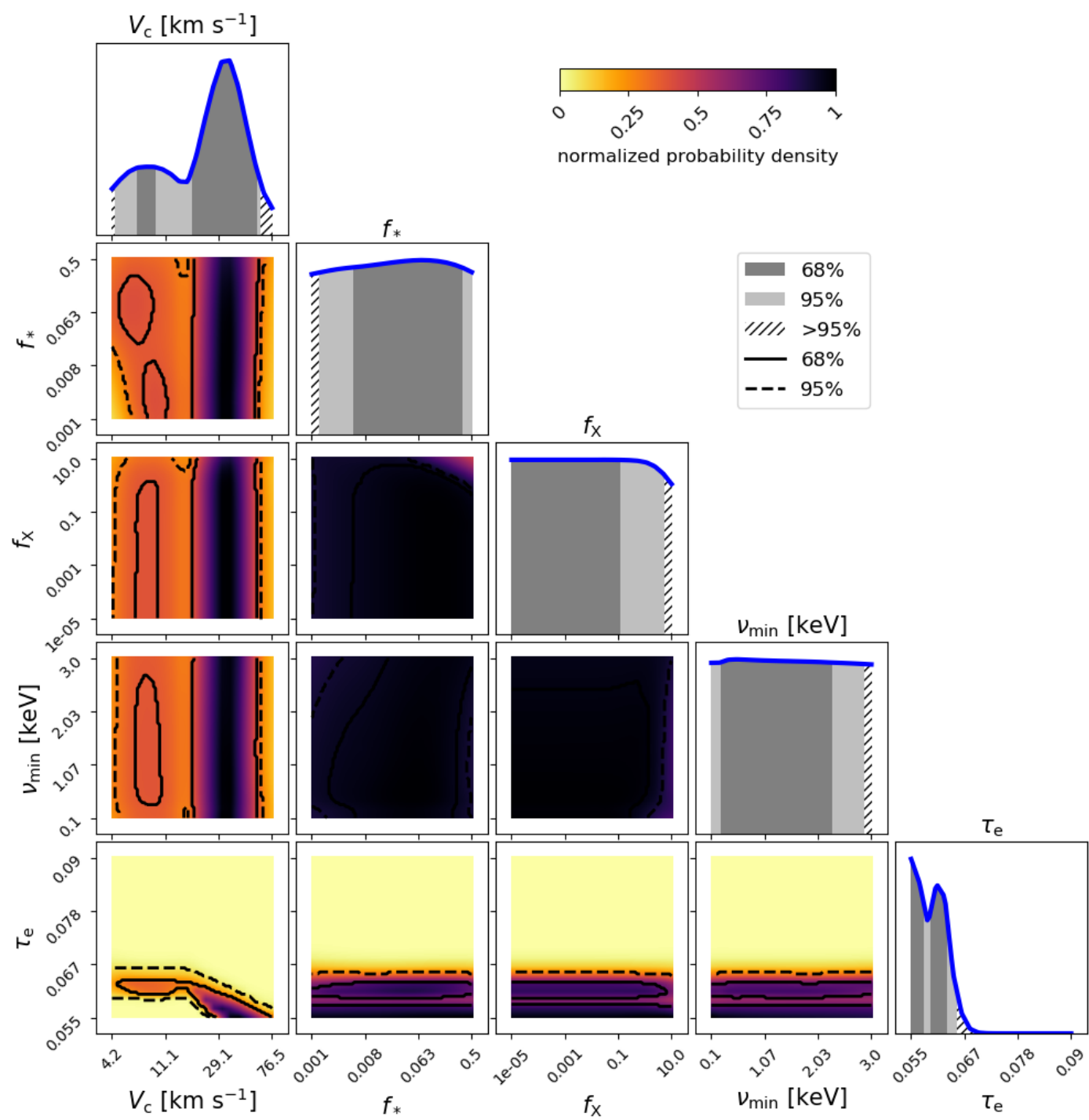
Monsalve, Fialkov, et al. (2019)

EDGES High-Band

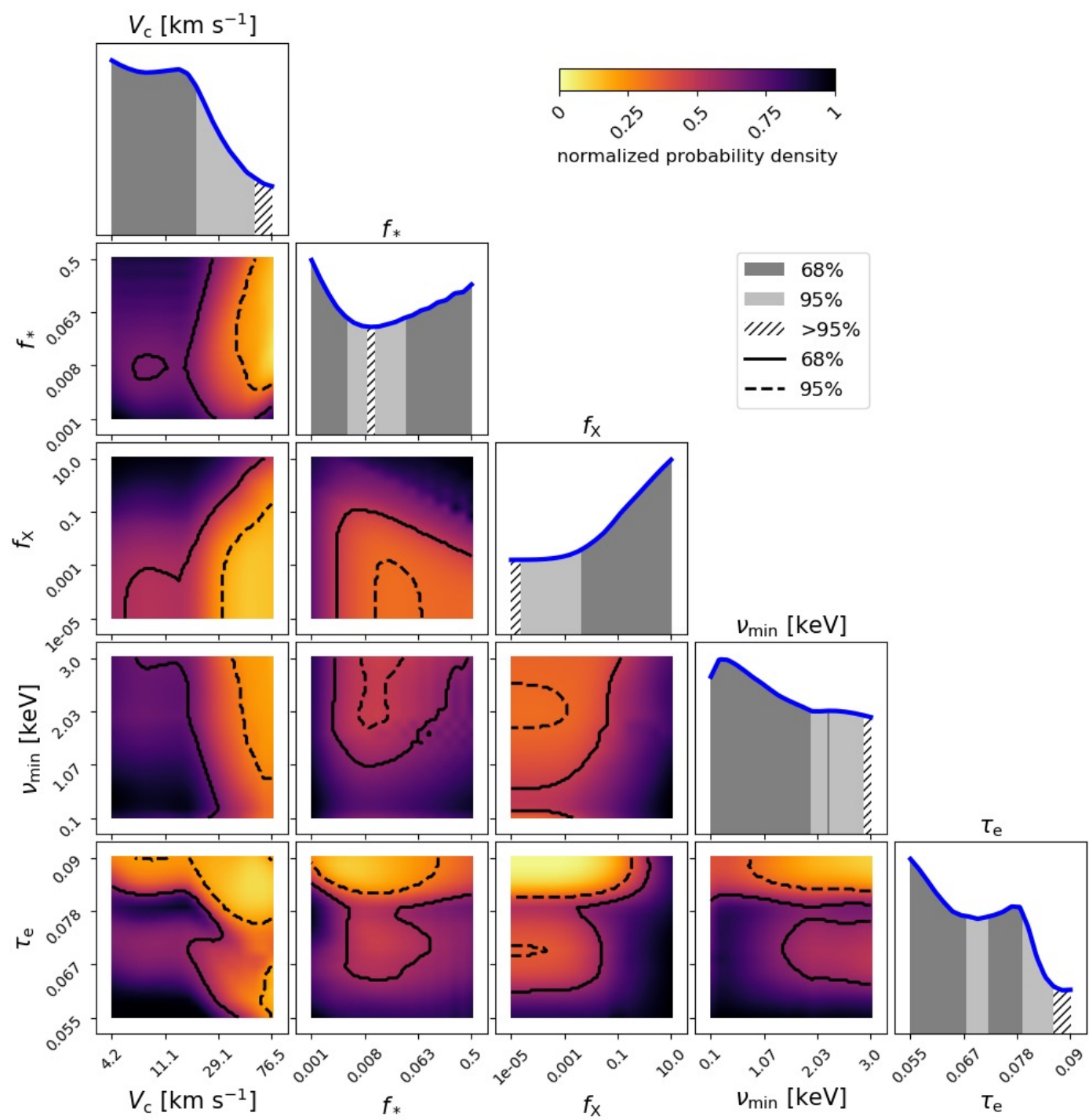
External Priors



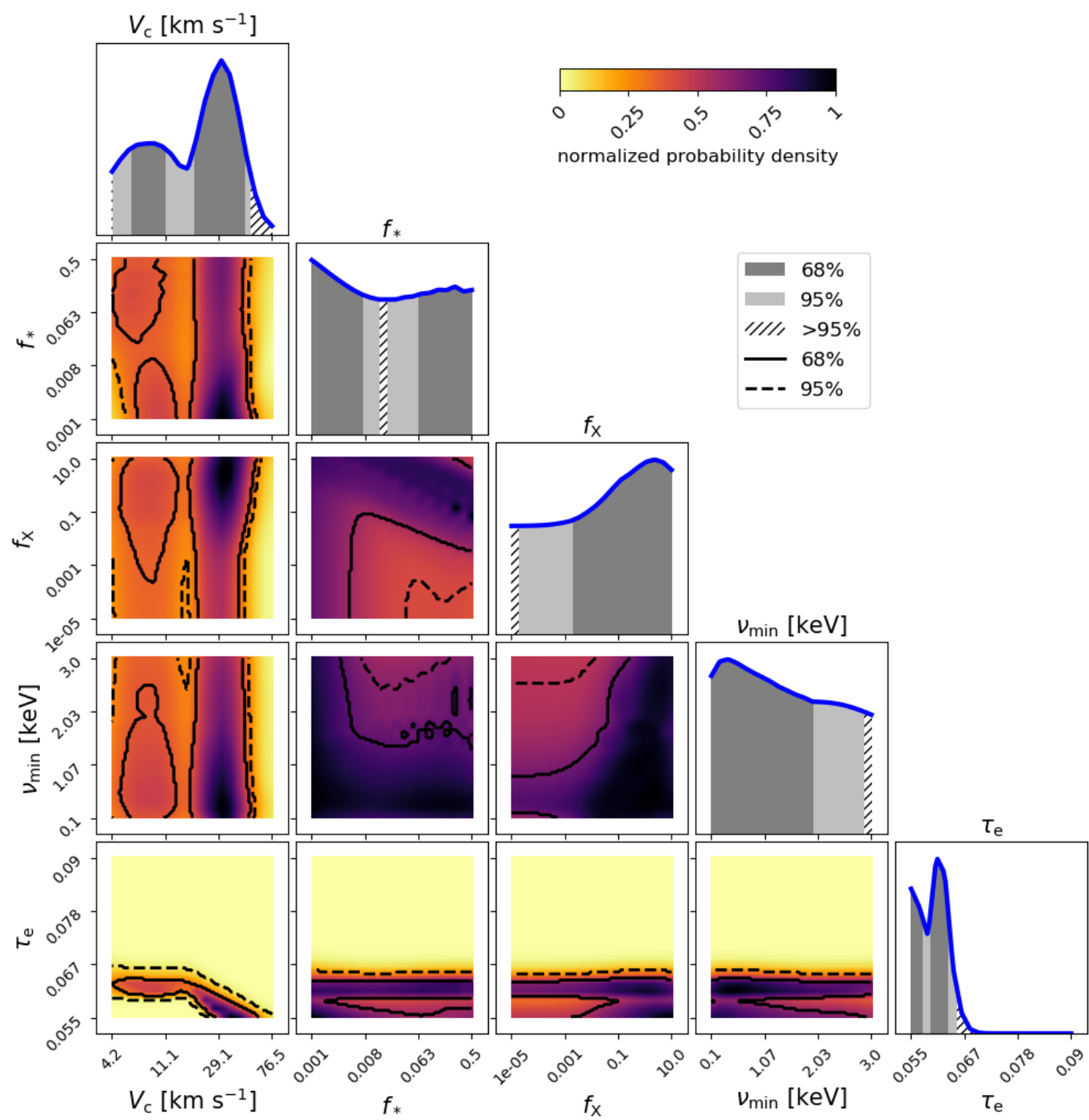
Constraints from External Priors



Constraints from EDGES High-Band



Constraints from External Priors + EDGES High-Band

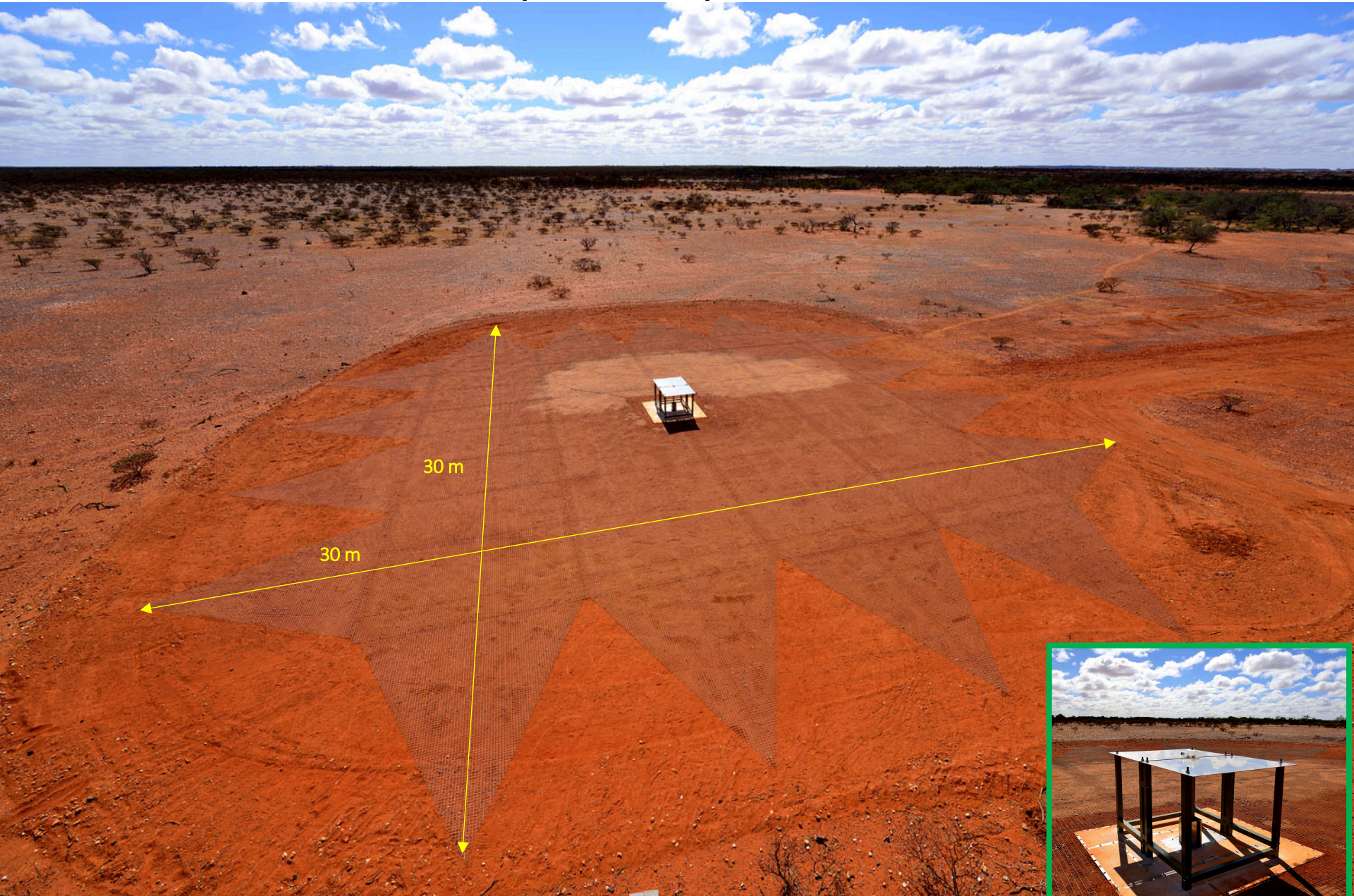


Monsalve, Greig, et al. (2018)

Likelihood of 21-cm models computed after marginalizing over linear foreground parameters

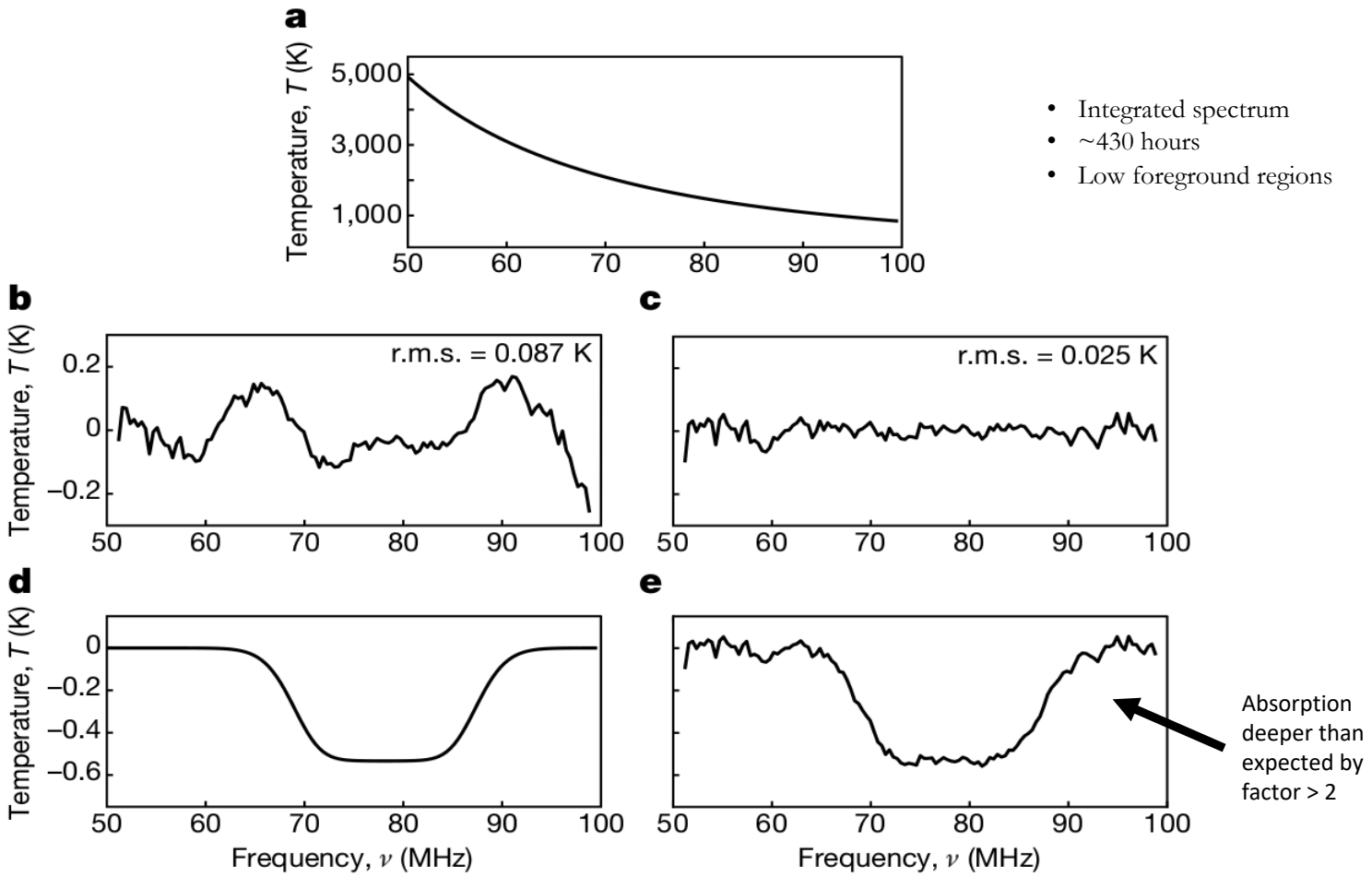
$$\begin{aligned}\mathcal{L}(d|\boldsymbol{\theta}_{21}) &= \int \mathcal{L}(d|\boldsymbol{\theta}_{21}, \boldsymbol{\delta}_{\text{fg}}) d\boldsymbol{\delta}_{\text{fg}} \\ &= \sqrt{\frac{(2\pi)^{N_{\text{fg}}-N_{\nu}}}{|\boldsymbol{\Sigma}||\boldsymbol{C}^{-1}|}} \exp \left\{ -\frac{1}{2} d_{\star}^T (\boldsymbol{\Sigma} + \boldsymbol{V})^{-1} d_{\star} \right\}\end{aligned}$$

Bowman et al. (2018)



Bowman et al. (2018)

Nominal



Bowman et al. (2018)

How to Explain Deep Absorption?

$$T_b(z) \propto \left(1 - \frac{T_{\text{CMB}} + T_{\text{EXCESS}}}{T_S} \right)$$

Suggested sources:

- Radio emission from **early black holes** (Ewall-Wice et al. 2018)
- Decay of **unstable particles** (Pospelov et al. 2018) (Aristizabal Sierra & Sheng Fong 2018)

Lower than expected

T_K Lower than expected

Suggested source:

- Interactions between **Baryons and Dark Matter** particles (Muñoz & Loeb 2018)

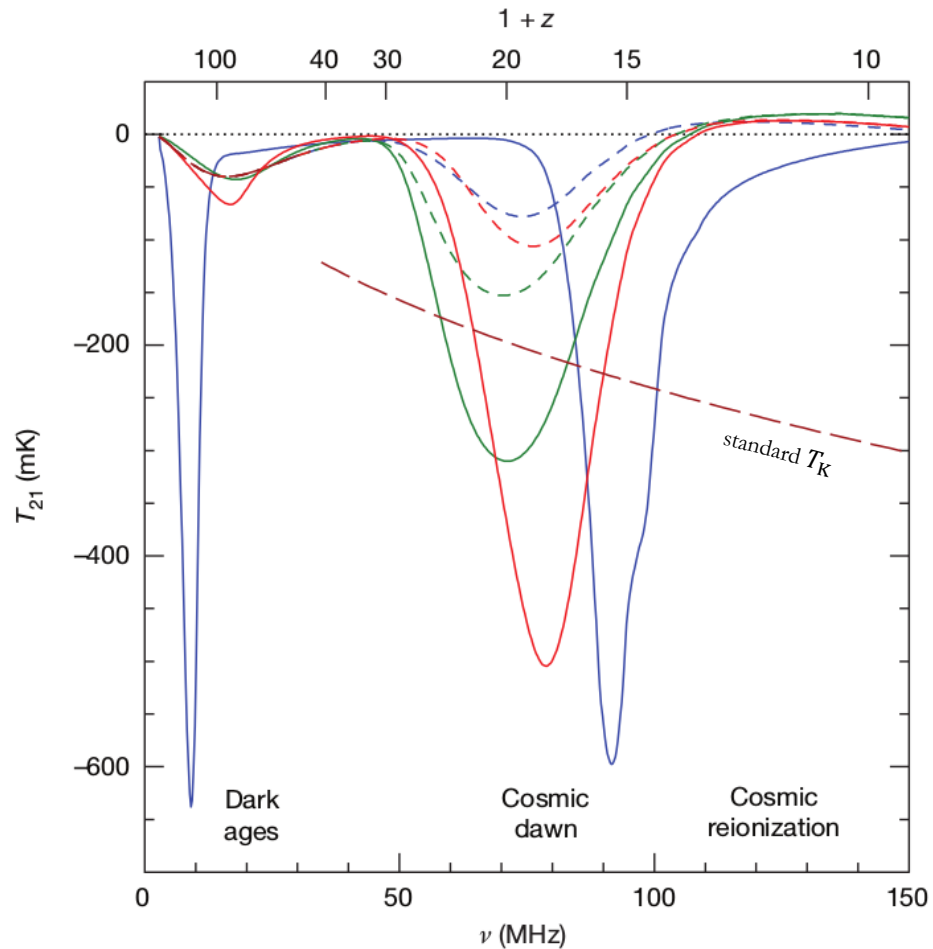
Bowman et al. (2018)

Interaction of Baryons with Dark Matter?

Enough IGM cooling can be achieved if (Muñoz & Loeb 2018):

- $\sim 1\%$ of DM particles
- have mass $\sim 1\text{-}60$ MeV
- and possess electric mini-charge, $\sim 10^{-6}$ the charge of an electron

Possibility of non-gravitational interaction between baryons and dark matter.



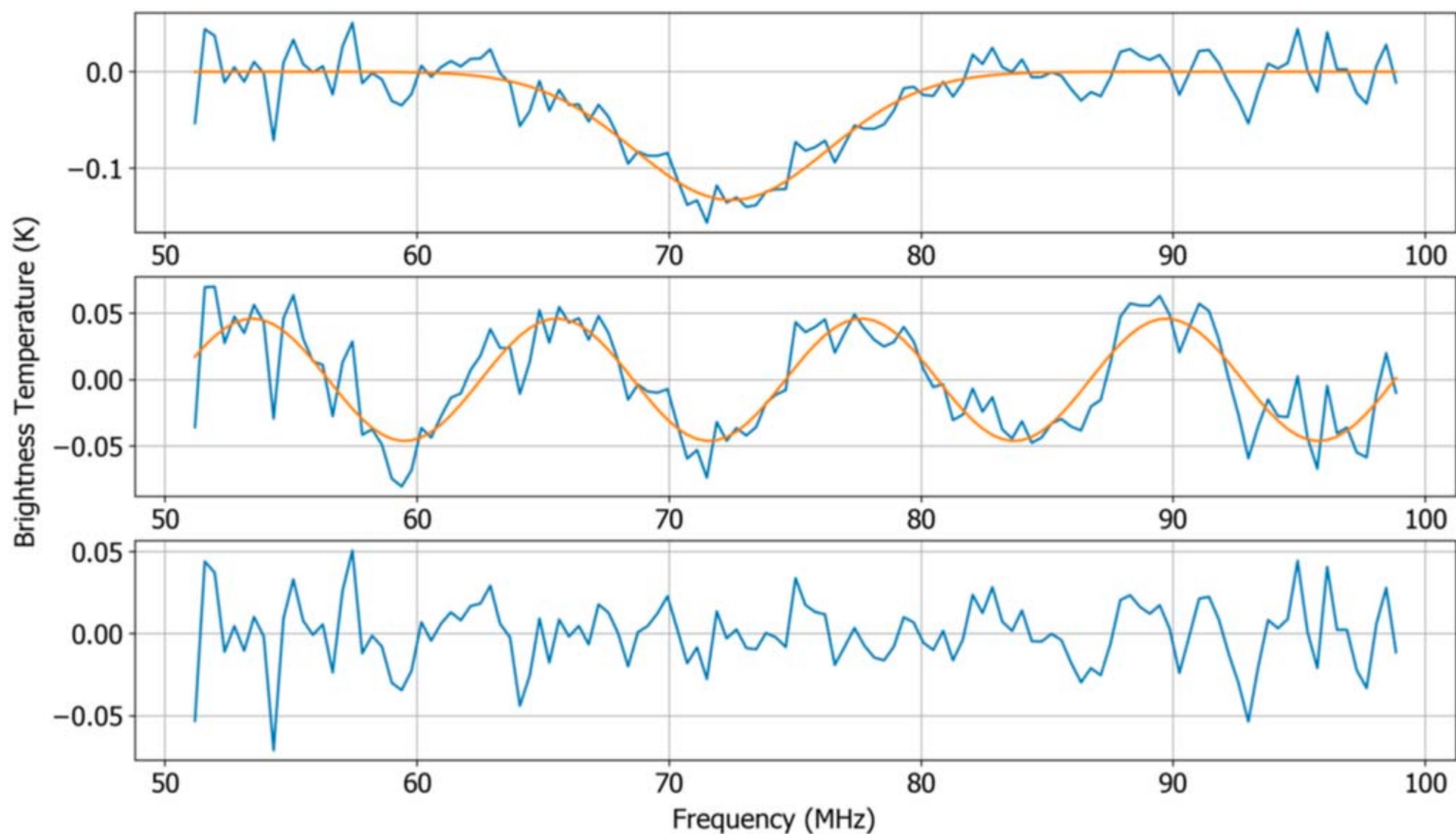
R. Barkana 2018, **Nature**, 555, 71

The Redshifted 21 cm Signal in the EDGES Low-band Spectrum

Saurabh Singh^{1,2,3} and Ravi Subrahmanyan³ 

(2019)

- MS + Sinusoid + Gaussian
- Best-fit Gaussian has “standard” amplitude
- Lower residuals RMS
- Lower BIC

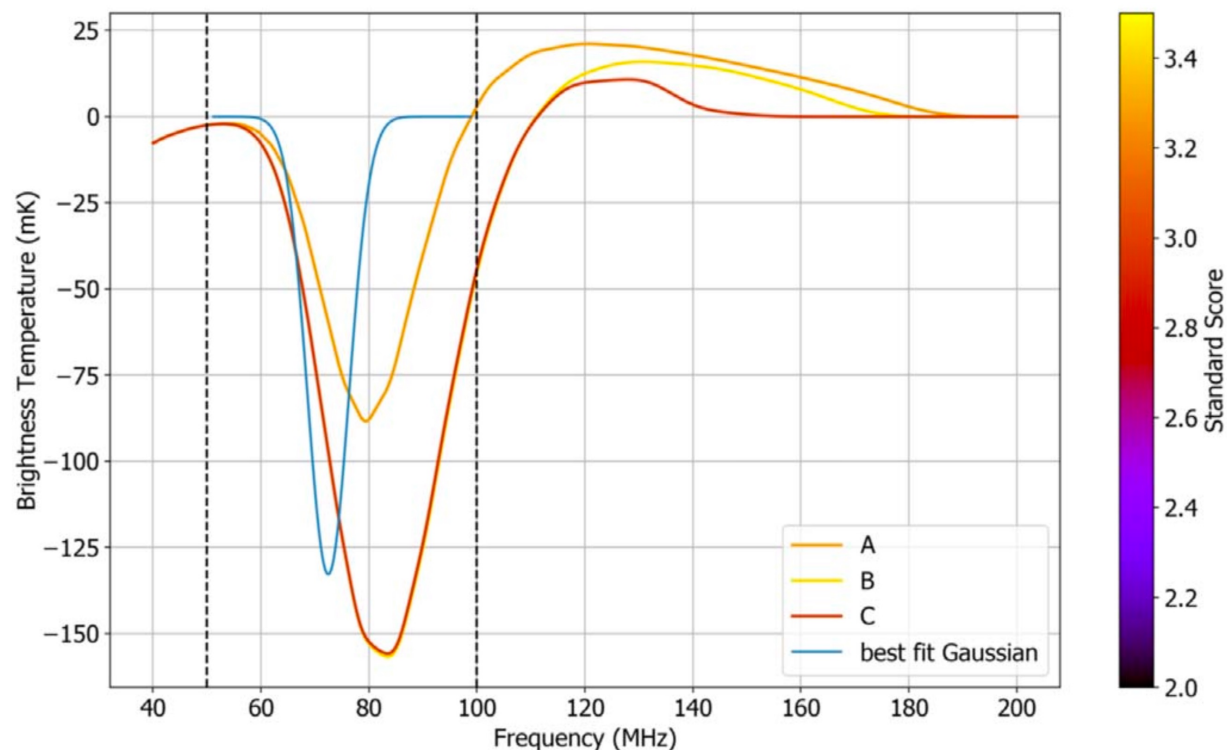


The Redshifted 21 cm Signal in the EDGES Low-band Spectrum

Saurabh Singh^{1,2,3} and Ravi Subrahmanyan³ 

(2019)

- MS + Sinusoid + (scale x template)
- Template from Cohen et al. (2017)



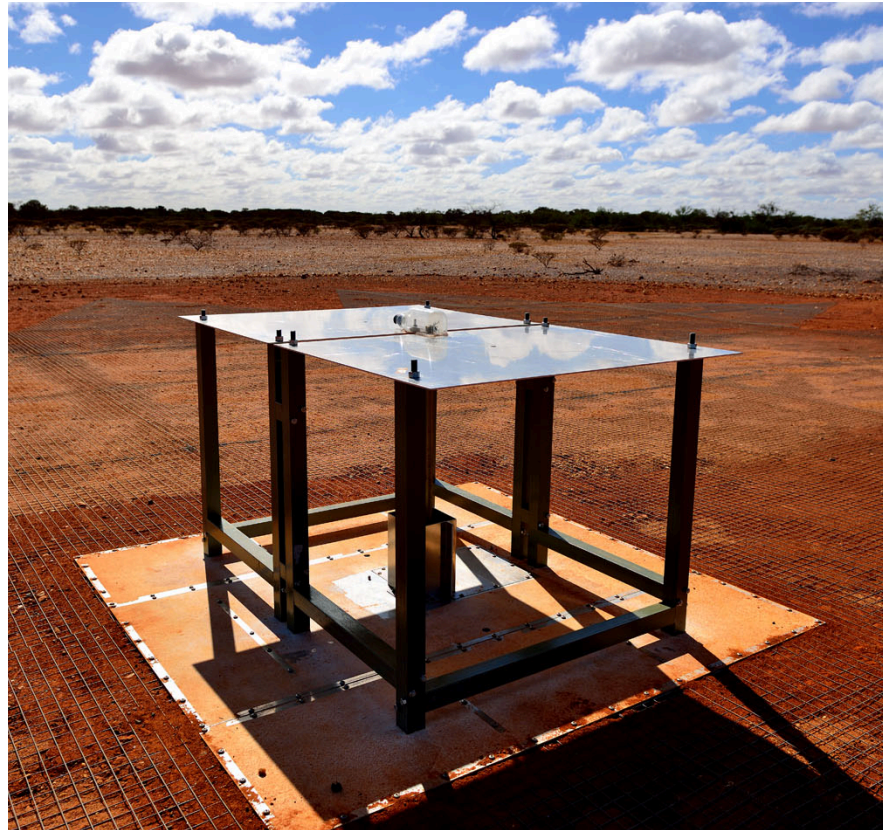
Parameters of the 21 cm Signals Favored by the Data

Case	f_*	V_c (km s ⁻¹)	f_X	τ	R_{mfp} (Mpc)
A	0.05	35.50	14.7	0.061	70
B	0.158	35.50	1.58	0.066	70
C	0.158	35.50	1.58	0.082	70

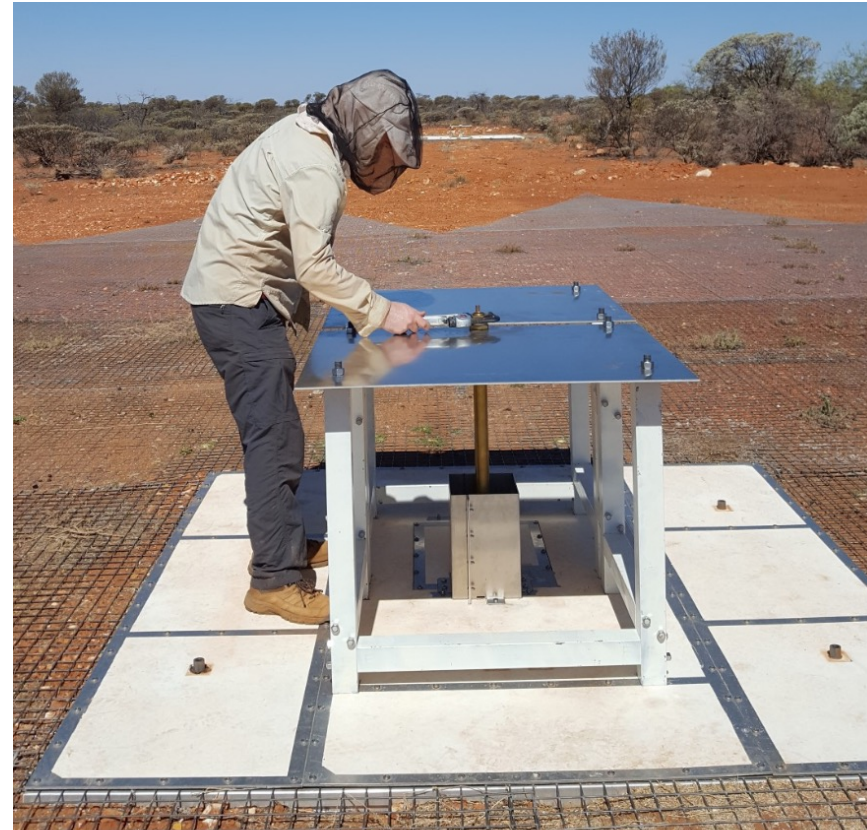
EDGES-2 in 2018-2020

Verification with EDGES-2 Mid-Band

Low-Band



Mid-Band (~25% smaller)



Same Ground Plane as Low-Band

Objective:

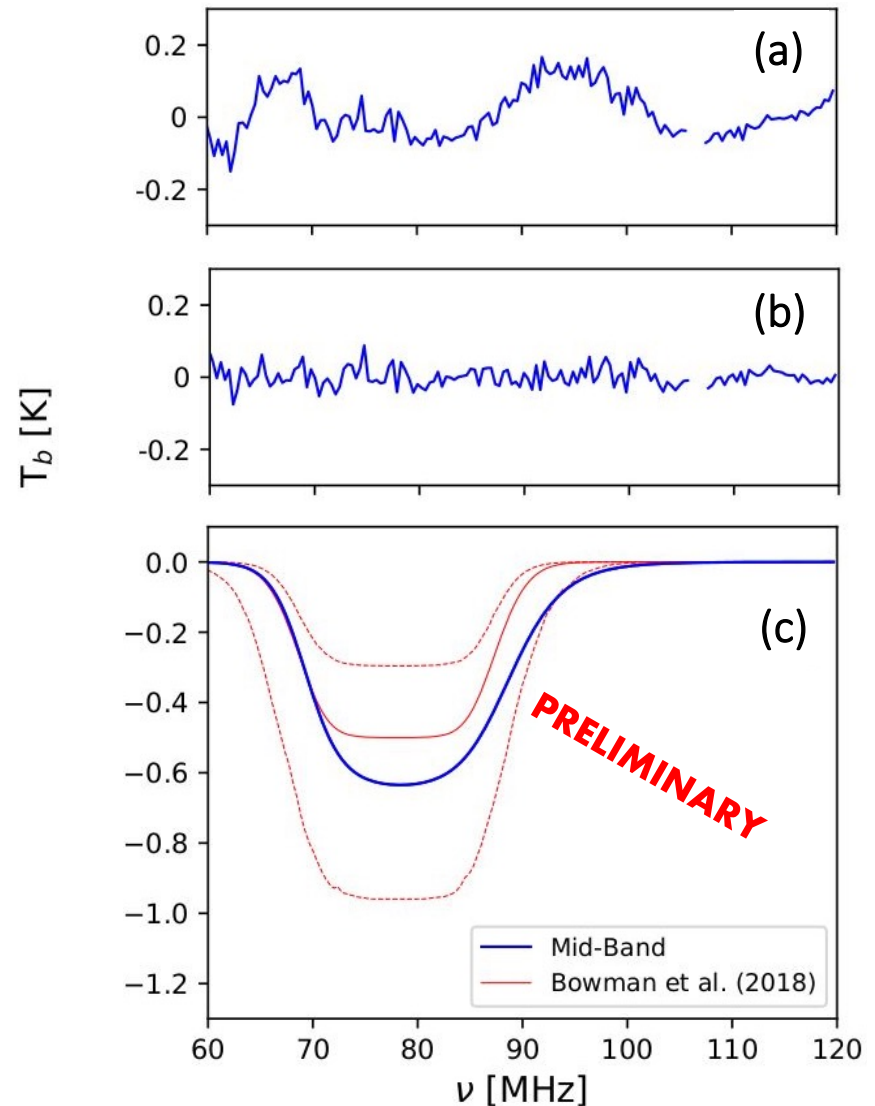
Shift some of the spectral structures from the instrument to higher frequencies

EDGES-2 in 2018-2020

Verification with EDGES-2 Mid-Band

For many data cuts,
adding a flattened Gaussian absorption model
consistent with Bowman et al. (2018) **improves the fit.**

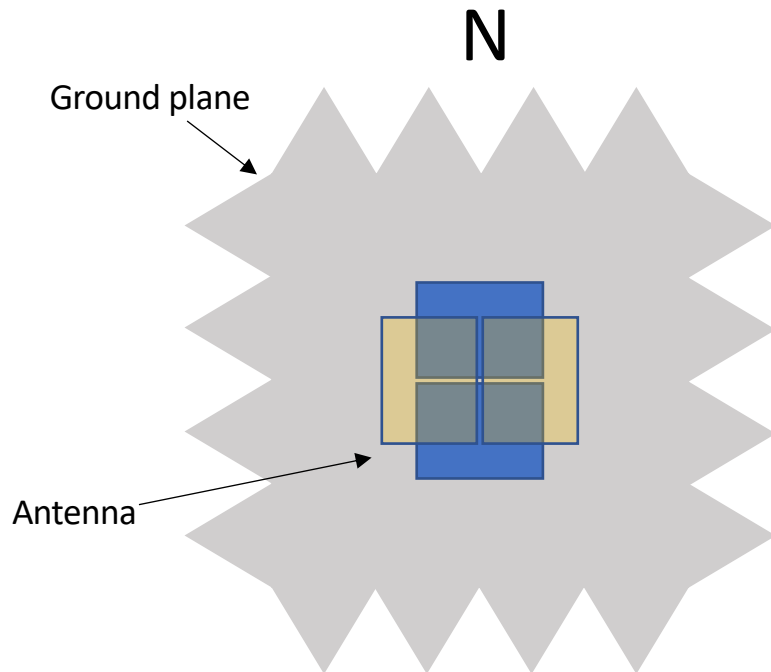
Bayesian pipeline is being written to analyze all the aspects of
the experiment in a statistically robust and self consistent way



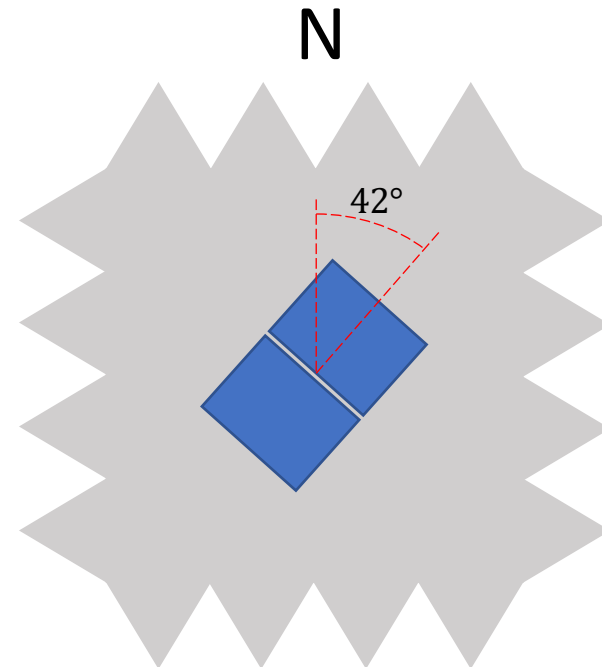
EDGES-2 in 2018-2020

Verification with EDGES-2 **Rotated Low-Band**

Low-Band **before 2020**



Low-Band **in 2020**

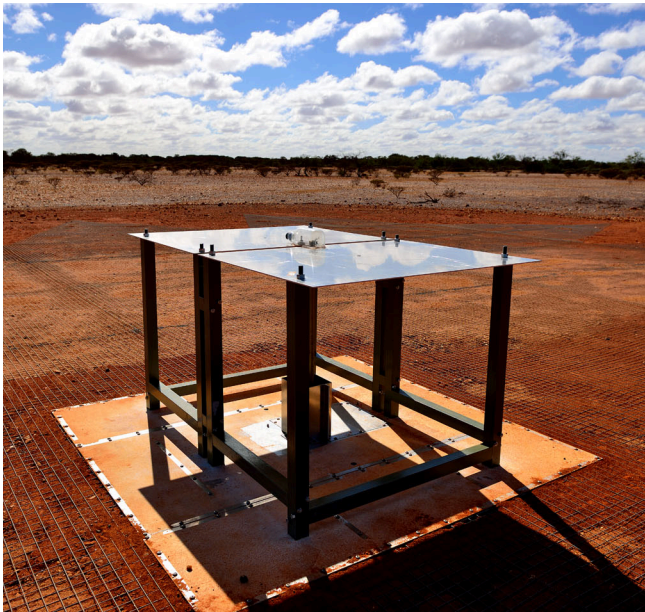


Different EM interaction between antenna and ground plane

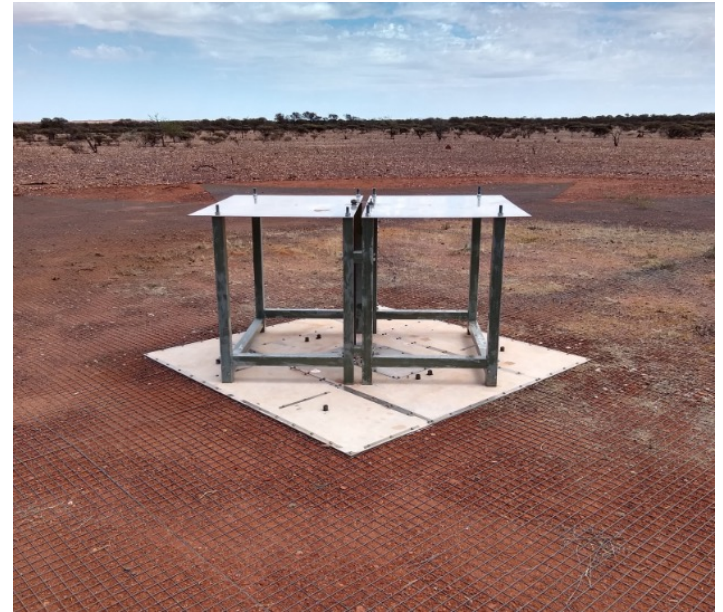
EDGES-2 in 2018-2020

Verification with EDGES-2 **Rotated Low-Band**

Low-Band



Rotated Low-Band

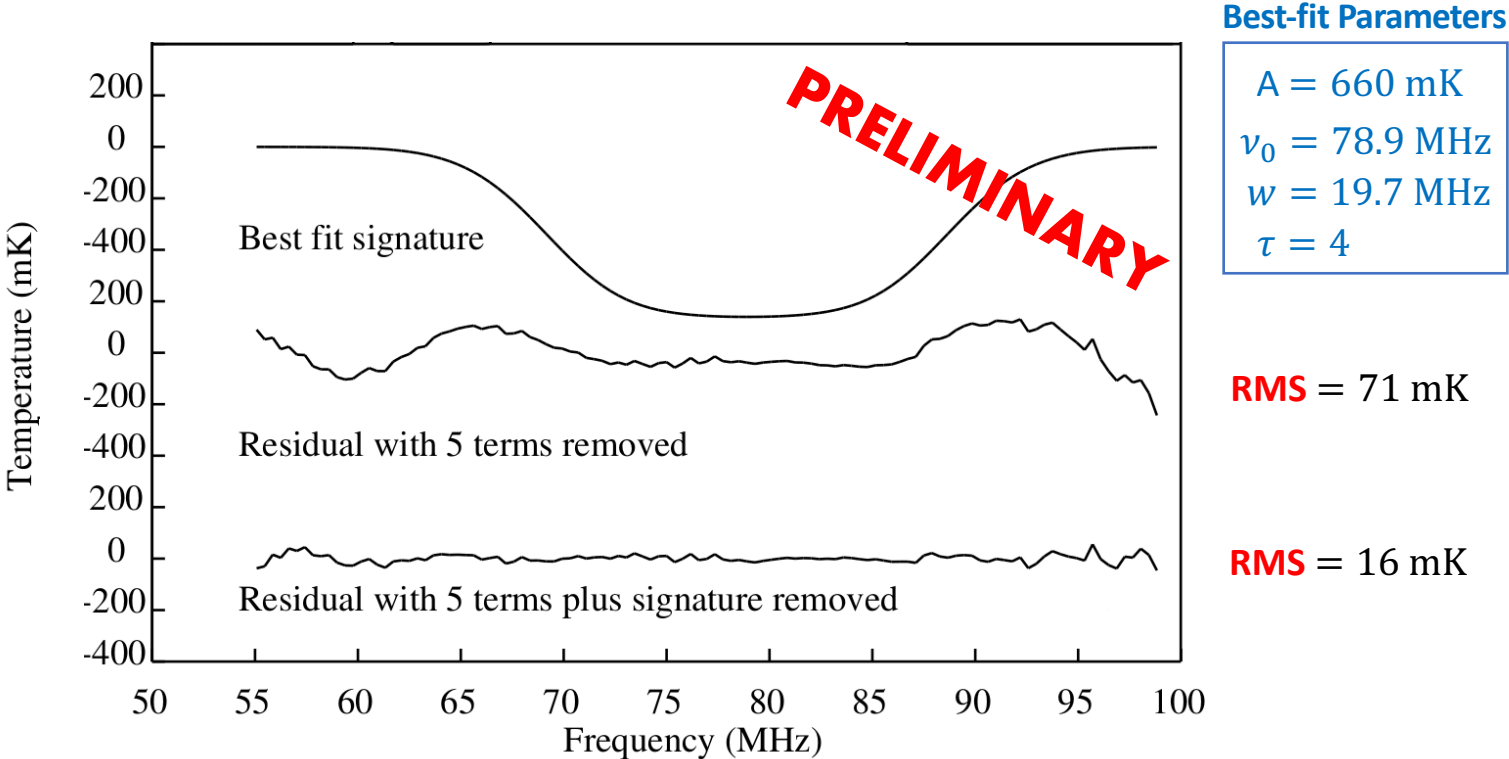


Objective:

Change the spectral structures from interaction between antenna and ground plane

EDGES-2 in 2018-2020

Verification with EDGES-2 Rotated Low-Band



For many data cuts, adding a flattened Gaussian absorption model consistent with Bowman et al. (2018) **improves the fit.**

Bayesian pipeline is being written to analyze all the aspects of the experiment in a statistically robust and self consistent way

Recent progress by SARAS+

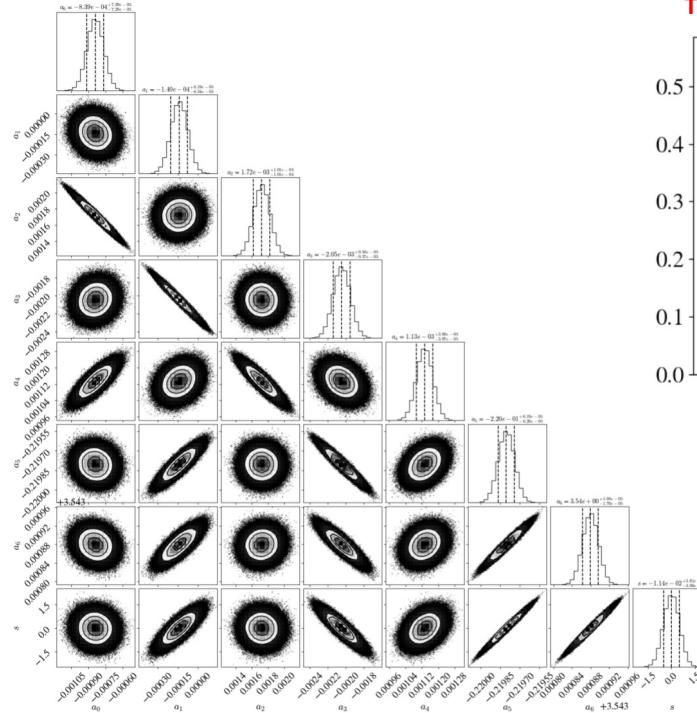
On the detection of a cosmic dawn signal in the radio background

(2022)

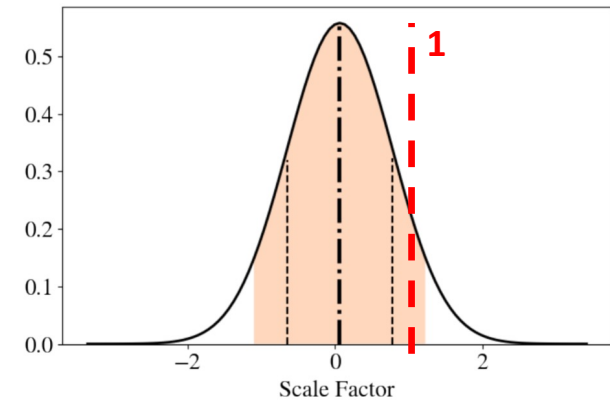
Saurabh Singh ^{1,2,3} ✉, Jishnu Nambissan T.^{1,4}, Ravi Subrahmanyam ^{1,5}, N. Udaya Shankar¹,
B. S. Girish ¹, A. Raghunathan ¹, R. Somashekar ¹, K. S. Srivani ¹ and Mayuri Sathyanarayana Rao ¹



SARAS 3 on a lake in India



The value of 1 is within 90% confidence range.



90% confidence range for scale, considering systematics and range of EDGES signals.

- 55-85 MHz band modeled with:
 - 7-term log-log polynomial
 - + 1 scale factor for best-fit EDGES signal

A comprehensive Bayesian reanalysis of the SARAS2 data from the epoch of reionization

(2022)

H. T. J. Bevins¹*, E. de Lera Acedo^{1,2}, A. Fialkov^{2,3}, W. J. Handley^{1,2}, S. Singh^{4,5,6},
R. Subrahmanyan⁷ and R. Barkana^{8,9}

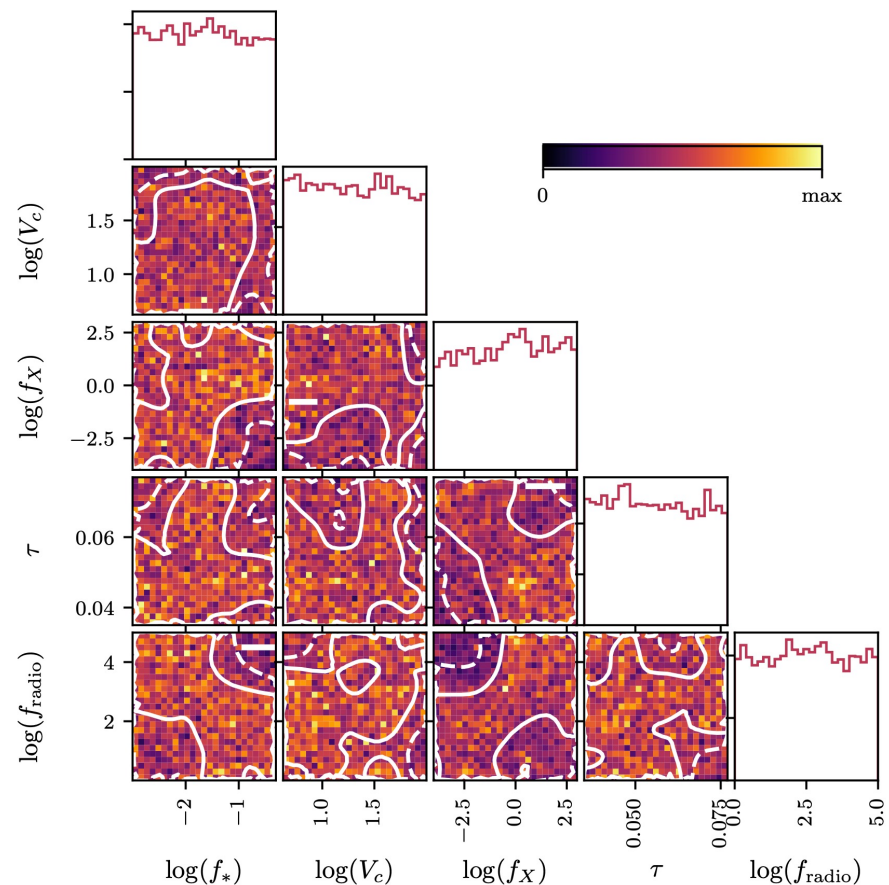
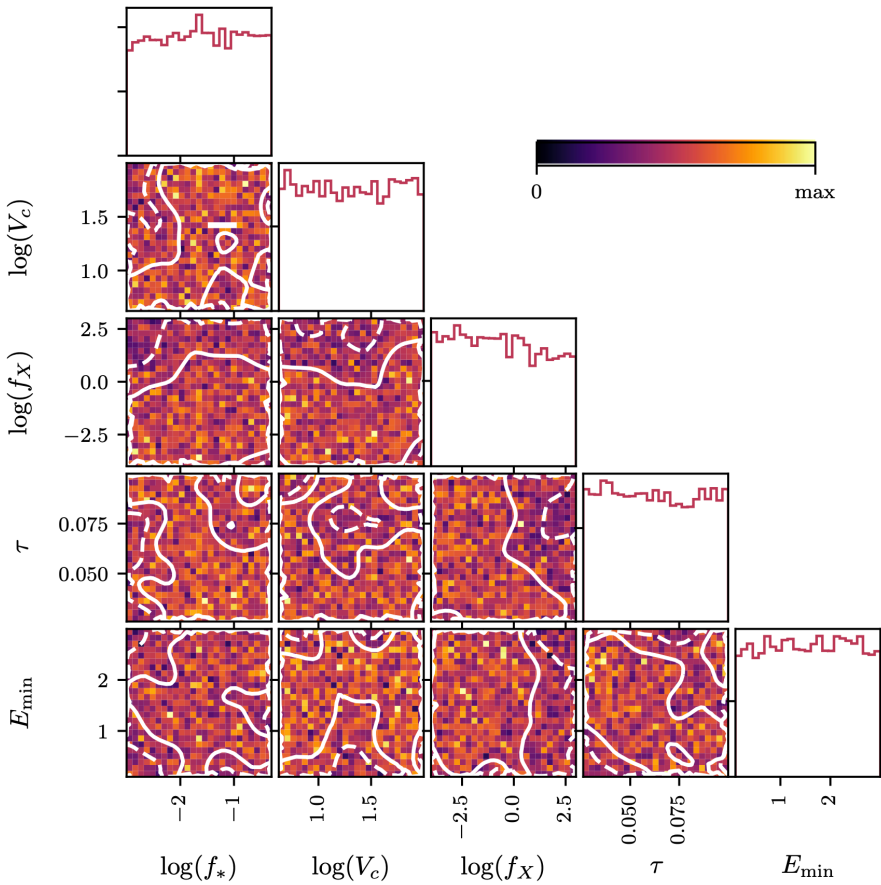
Fitting the foreground with a “partially smooth function” suggests that there is a sinusoidal systematic

	Parameter	Prior	Prior type
Systematic	α_{sys}	0–10	Uniform
	A	0–1 K	
	P	10–70 MHz	
	ϕ	0– 2π rad	
Signal	τ	0.026–0.1 (STA) / 0.035–0.077 (ERB)	Uniform
	α	1.3 (STA only)	
	E_{min}	0.1–3 keV (STA only)	
	R_{mfp}	30 (STA) / 40 (ERB) Mpc	
	f_*	0.001–0.5	Log-Uniform
	V_c	4.2–100 km s ⁻¹	
	f_X	0.0001–1000	
	f_{radio}	1–99 500 (ERB only)	

A comprehensive Bayesian reanalysis of the SARAS2 data from the epoch of reionization




(2022)

H. T. J. Bevins¹*, E. de Lera Acedo^{1,2}, A. Fialkov^{2,3}, W. J. Handley^{1,2}, S. Singh^{4,5,6},
R. Subrahmanyan⁷ and R. Barkana^{8,9}



Astrophysical constraints from the SARAS 3 non-detection of the cosmic dawn sky-averaged 21-cm signal

Received: 10 May 2022



H. T. J. Bevens^{1,2}  , A. Fialkov^{2,3}, E. de Lera Acedo^{1,2}, W. J. Handley^{1,2}, S. Singh⁴, R. Subrahmanyan⁵  & R. Barkana^{6,7,8} 

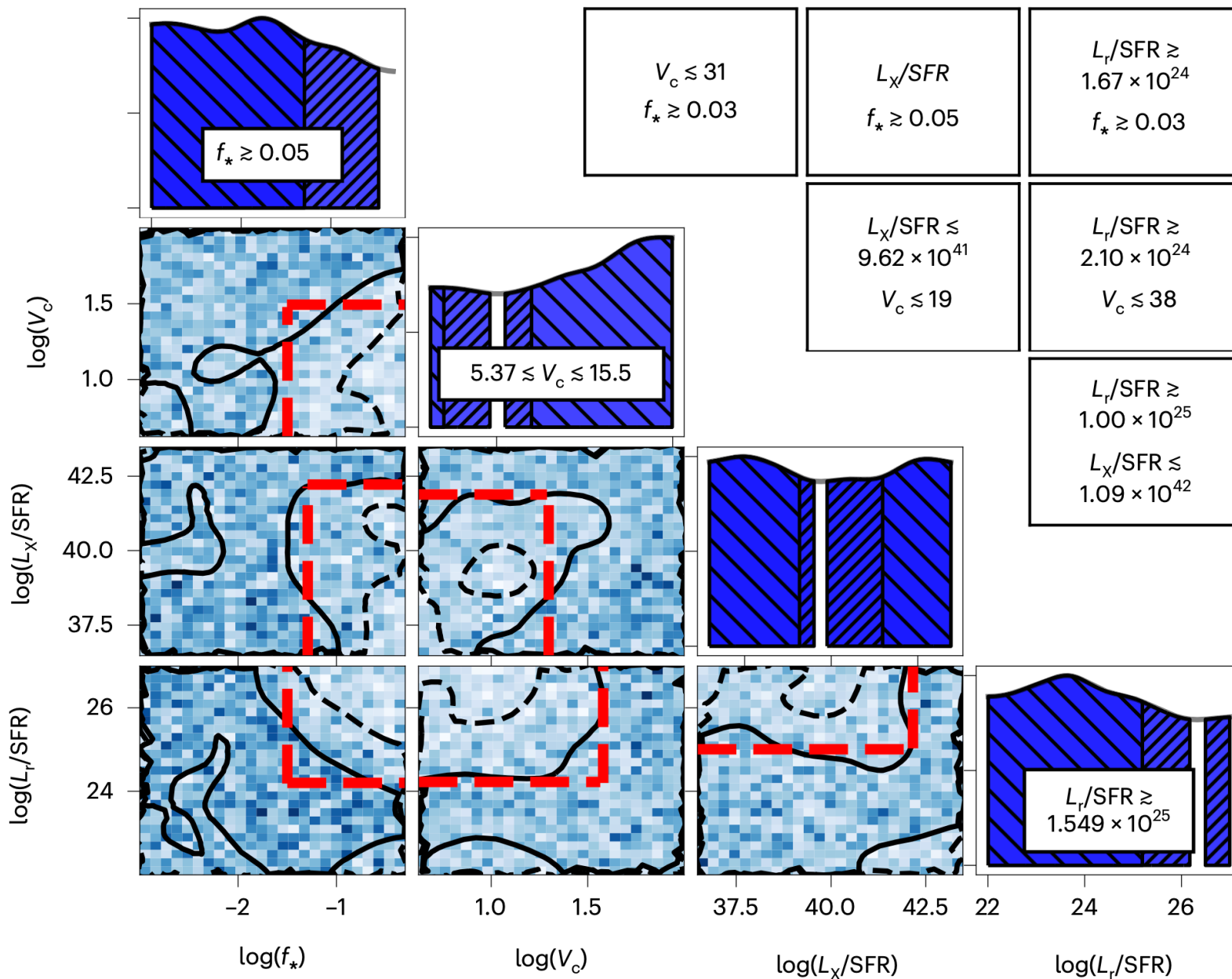
Accepted: 21 September 2022

Fitting the foreground with a 7-term log-log polynomial

Table 2 | The astrophysical priors

Parameter	Radio background	Range
f_*	CMB only, synchrotron, radio galaxies	0.001–0.5
V_c (km s ⁻¹)	CMB only, synchrotron, radio galaxies	4.2–100
f_x	CMB only, synchrotron, radio galaxies	0.001–1,000
f_{radio}	Radio galaxies	1.0–99,500
$A_r^{1,420}$	Synchrotron	0–47
τ	CMB only	0.026–0.103
	Synchrotron	0.016–0.158
	Radio galaxies	0.035–0.077
α	CMB only	1.0–1.5
E_{min} (keV)	CMB only	0.1–3.0
R_{mfp} (Mpc)	CMB only, synchrotron, radio galaxies	Fixed at 30, 40 and 40

 95% confidence
 68% confidence



Astrophysical constraints from the SARAS 3 non-detection of the cosmic dawn sky-averaged 21-cm signal

Received: 10 May 2022

H. T. J. Bevens^{1,2}✉, A. Fialkov^{2,3}, E. de Lera Acedo^{1,2}, W. J. Handley^{1,2}, S. Singh⁴, R. Subrahmanyam⁵ & R. Barkana^{6,7,8}

Accepted: 21 September 2022

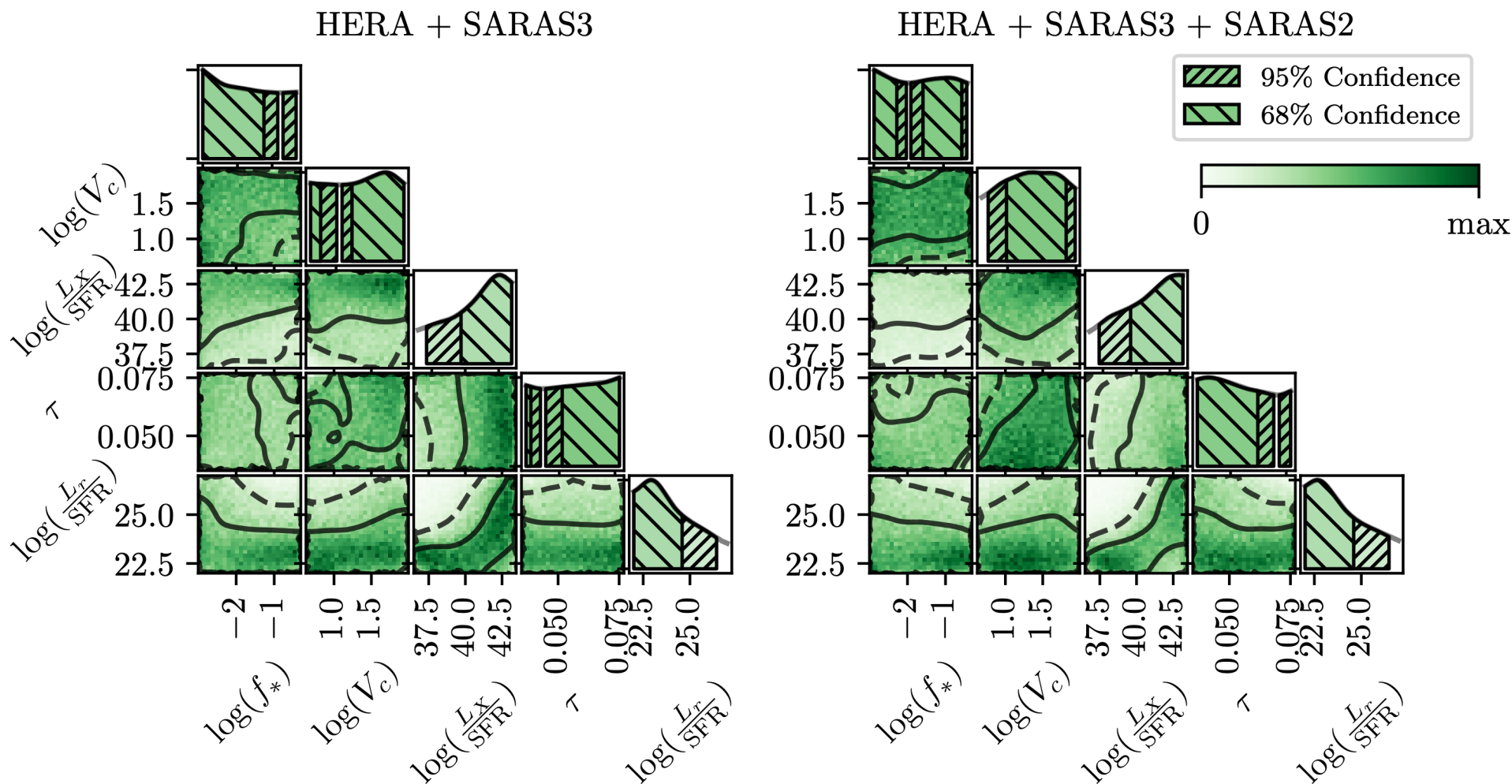
Table 3 | Summary of key constraints from SARAS 3 (this work), HERA and SARAS 2 experiments

	SARAS 3	HERA	SARAS 2
Signal type	Global	Power spectrum	Global
Redshift range	$z \approx 15\text{--}25$	$z \approx 8$ and $z \approx 10$	$z \approx 7\text{--}12$
L_{ν}/SFR ($\text{WHz}^{-1}M_{\odot}^{-1}\text{yr}$)	$\gtrsim 1.549 \times 10^{25}$	$\gtrsim 4.00 \times 10^{24}$	–
$L_{\nu}/\text{SFR} \cap L_{\nu}/\text{SFR}$ ($\text{ergs}^{-1}M_{\odot}^{-1}\text{yr}$)	$\gtrsim 1 \times 10^{25} \cap \lesssim 1.09 \times 10^{42}$	$\gtrsim 4.00 \times 10^{24} \cap \lesssim 7.60 \times 10^{39}$	$\gtrsim 4.07 \times 10^{24} \cap \lesssim 6.3 \times 10^{39}$
M (M_{\odot})	$4.4 \times 10^5 \lesssim M \lesssim 1.1 \times 10^7$	–	–
f_{\ast}	$\gtrsim 0.05$	–	–
$f_{\ast} \cap M$ (M_{\odot})	$\gtrsim 0.03 \cap \lesssim 8.53 \times 10^8$	–	–

Joint analysis constraints on the physics of the first galaxies with low frequency radio astronomy data

(2023)

Harry T. J. Bevins^{1,2}★, Stefan Heimersheim³, Irene Abril-Cabezas³, Anastasia Fialkov^{2,3}, Eloy de Lera Acedo^{1,2}, William Handley^{1,2}, Saurabh Singh⁴ and Rennan Barkana^{5,6}



Thank You Very Much